Association Euratom - Risø National Laboratory annual progress report 2002

Bindslev, Henrik; Singh, B.N

Publication date:
2003

Document Version
Publisher's PDF, also known as Version of record

Risø-R-1414(EN)

Association Euratom - Risø National Laboratory Annual Progress Report 2002

Edited by H. Bindslev and B.N. Singh

Risø National Laboratory
May 2003

Abstract The programme of the Research Unit of the Fusion Association Euratom - Risø National Laboratory covers work in fusion plasma physics and in fusion technology. The fusion plasma physics research focuses on turbulence and transport, and its interaction with the plasma equilibrium and particles. The effort includes both first principles based modelling, and experimental observations of turbulence and of fast ion dynamics by collective Thomson scattering. The activities in technology cover investigations of radiation damage of fusion reactor materials. These activities contribute to the Next Step, the Long-term and the Underlying Fusion Technology programme. A summary is presented of the results obtained in the Research Unit during 2002.

ISBN 87-550-3225-7
ISBN 87-550-3226-5 (Internet)
ISSN 0106-2840; 1396-3449

Foreword

Risø participates in the internationally coordinated activities to develop fusion as a major source of energy. The principle being pursued is the fusion of hydrogen isotopes to form helium. This is the process, which powers the sun. To make the fusion process run at a significant rate the hydrogen gas must be heated to high temperatures where it ionises and turns into a plasma. Furthermore, the plasma must be confined to achieve suitable densities and sustain the high temperature. On the sun gravity provides the confinement. On earth, the line we are pursuing, use a magnetic field for the confinement. While fusion holds the promise of providing a sustainable source of energy, which is environmentally sound, it also presents considerable scientific and engineering challenges. Key issues in the final steps towards realising fusion energy production include:

1. Improving the plasma energy confinement, that is the ratio between the energy of the plasma and the heating power required to sustain the plasma energy. Improving energy confinement implies reducing energy transport out of the plasma, which principally is due to turbulence. So what we really need to do is to understand and control turbulence.
2. Channelling the energy of fast ions, produced in fusion reactions, into heating the bulk plasma without driving turbulence and without premature exit of the fast ions from the plasma. This requires understanding and control of the dynamics of the fast ions in interaction with other particles and with waves.
3. Development of materials, which maintain required mechanical properties under high and sustained neutron fluxes. Neutrons, produced in the fusion reactions, are not confined by the magnetic field. They pass through the first wall of the chamber surrounding the plasma, slowing down on impact with atoms in the wall. The energy thus deposited generates cascades of atomic displacements in the first wall materials. The accumulation of surviving defects thus produced causes changes in the physical and mechanical properties of the materials exposed to the flux of fusion [14 MeV] neutrons.

Risø contributes to fusion research in all these areas: 1) codes, modelling turbulence and transport, have been developed and are continually improved, and benchmarked against experiments. Of particular note this year was the development of a two-dimensional edge tubulence model, which displays intermitent ejection of plasma blobs, reminiscent of the bursty behaviour of edge transport found in experiments. 2) Central to understanding the dynamics of fast ions is the acquisition of temporally and spatially resolved measurements of the fast ion velocity distributions in the plasma. Risø, in collaboration with MIT (USA) and EURATOM partners, is developing and operating millimetre wave based collective Thomson scattering diagnostics at the TEXTOR and ASDEX upgrade tokamaks in FZ-Jülich and the Max-Planck Institute for plasma physics in Garching (near Munich). 3) In the field of irradiated materials research Risø is investigating the properties of copper alloys relevant to the next step in fusion research, ITER, and of iron alloys, which will be an essential component of a demonstration/commercial fusion reactor.

Henrik Bindslev and B.N. Singh
Risø National Laboratory
April 2003

Contents

1. Summary of Research Unit activities

The activities in the Research Unit cover two main areas:

Fusion Plasma Physics, which includes:

- *Theoretical and numerical turbulence studies*. Turbulence and the associated anomalous transport is investigated using first principles based models and solving these by means of numerical codes in full toroidal geometry. These models are continuously being developed and benchmarked against existing codes at other associations. The dynamics of bursts of fluctuations leading to profile relaxation have been studied in models for flux-driven interchange mode turbulence, where the back reaction of the turbulence on the equilibrium flows and profiles are accounted for.
- *Fast Ion Collective Thomson Scattering.* Risø has taken the lead in the development of fast ion collective Thomson scattering diagnostics for TEXTOR and ASDEX upgrade (AUG). These projects are carried out in close collaborations with MIT, and with the TEC[†] and AUG teams.

Fusion Technology, which includes:

- Experimental and theoretical investigations of the effects of irradiation on the microstructural evolution and on the physical and mechanical properties of metals and alloys relevant to the Next Step, the Long Term and Underlying Fusion Technology Programme.

The **global indicators** for the Research Unit in 2002 are:

• Professional staff	11.3	man-years
• Support staff	6.9	man-years
• Total expenditure - incl. mobility	2.42	MioEuro
• Total Euratom support	0.75	MioEuro

[†] TEC: the Trilateral Euregio Cluster, a collaboration of FOM Institute for Plasma Physics, Holland; ERM/KMS, Belgium and Forschungszentrum Jülich, Germany.

2. Fusion plasma physics

2.1 Introduction

With steep gradients in plasma equilibrium parameters and with populations of energetic ions far from thermal equilibrium, fusion plasmas have considerable free energy. This energy drives turbulence, which in turn acts back on the equilibrium profiles and on the dynamics of the fast ions. The turbulence naturally gives rise to enhanced transport, but also sets up zonal flows that tear the turbulent structures apart and give rise to edge transport barriers; most likely at the root of the poorly understood, but experimentally reliably achieved high confinement mode (H-mode). This non-linear interplay between turbulence and equilibrium also supports transient events reminiscent of edge localized modes (ELMs) where energy and particles are ejected from the plasma edge in intermittent bursts.

This set of topics is the focus of our fusion plasma physics research: With first-principles based codes we seek to model the interplay between plasma turbulence, transport and equilibrium. This modelling is tested against experimental data in collaboration with other fusion plasma physics institutes. To elucidate the physics of fast ions and their interplay with turbulence, waves and transient events, we have engaged in a new activity, viz. the diagnosis of confined fast ions by collective Thomson scattering (CTS) at the TEXTOR tokamak in Forschungszentrum Jülich, Germany, and at the ASDEX upgrade tokamak in the Max-Planck Institute for Plasma Physics in Garching, Germany.

Our fusion plasma physics research programme provides fruitful collaborative projects with other academic groups working in non-linear science. A sign of the strength of these collaborative projects is that a member of our team heads the Research School in Nonlinear Science in Denmark.

2.2 Investigations on turbulence at the transition from edge to scrape-off layer

S. V. Annibaldi, F. Porcelli* (*Instituto Nazionale Fisica della Materia Torino, Italy),*
V. Naulin and J. Juul Rasmussen
volker.naulin@risoe.dk

Classical plasma turbulence and transport investigations usually deal with either closed magnetic field lines (edge) or open magnetic field lines that exclusively end on material interfaces (scrape-off Layer, SOL). Here we investigate the transition from closed to open field lines in a minimal model of the development of the plasma turbulence.

From the centre of the plasma the density decays to very low values at the material walls. The traditional approach to separate the turbulence into small perturbations and a background, determined by some equilibrium, is thus not feasible. Therefore the plasma dynamics has to be described by global dynamical equations taking into account variations in the magnetic field strength and variation of parameters such as collision frequencies. Moreover, the simulations have to cover the long transport timescale and still resolve the timescale of the turbulence, which demands good computational resources. Investigations on test-particle transport in this kind of turbulence have been planned and will also address the problem of inward transport of impurities.

Preliminary results show the evolution of a self-consistent density profile as depicted in Figure 1. The drop of density and fluctuation level in the SOL is due to plasma streaming to the limiter plates. The development of a presheath-like potential structure is visible. The transport in these systems is extremely bursty and the development of localized structures in the SOL, as already observable in a reduced 2D model (see 2.3) will be investigated in the future.

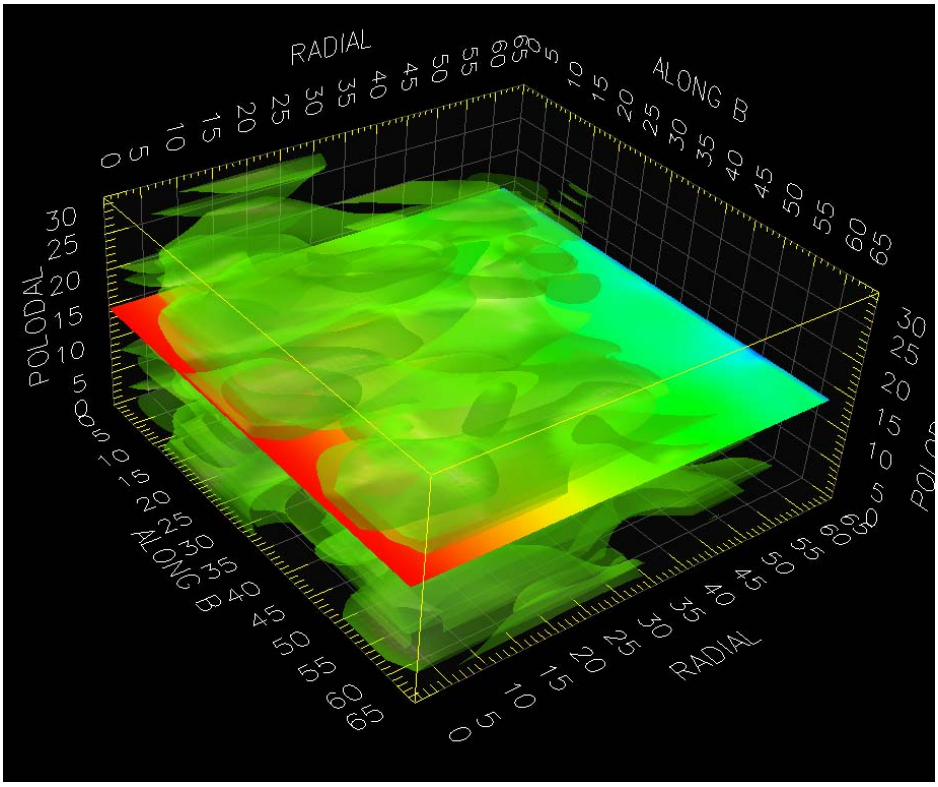

Figure 1. 3D visualisation of density fluctuations. The amplitude of the fluctuations stays relatively constant until the SOL, where they vanish. The plane shows a colour-code of the density, falling off towards the SOL. You should keep in mind that the length along the magnetic field is reduced by a factor of hundred. A high correlation of the fluctuations along the magnetic field is obvious.

2.3 Transport barriers and blobs in flute mode turbulence

A.H. Nielsen, V. Naulin and J. Juul Rasmussen
anders.h.nielsen@risoe.dk

We have investigated the evolution and dynamics of transport barriers in the form of zonal flows in a self-consistent model of pressure-driven electrostatic turbulence of a plasma in an inhomogeneous magnetic field. This is a simplified model of the outboard side of a toroidal confinement device. It captures the effects of unfavourable curvatures in an energy-preserving manner and describes the evolution of profiles as well as fluctuations.[1]

The model is solved numerically on a two-dimensional domain bounded in the radial direction and is periodic in the poloidal direction. The poloidal periodicity length is related to the safety factor. Near the inner wall in the radial direction we have included a source of plasma with a constant production rate and a fixed temperature. In the outer part of the domain, open magnetic field lines and thus a scrape-Off Layer (SOL), are simulated by

including local damping terms that model the losses of density, heat and charge to the limiter or divertor plates.

In Figure 2 we have depicted the evolution of the temperature field and we observe the formation of a blob of strong heat perturbation moving through the SOL. During the simulation temperature, density and vorticity pile up on the left-hand side of the domain, where the sources of density and heat are located. The radial gradients of these quantities are continuously increasing. At some point in time these gradients become unstable and the flow ejects a significant part of the plasma in the form of a concentrated blob into the SOL, where the plasma is lost. These blobs can propagate through the entire extent of the SOL and hit the outer wall, which makes their properties and the statistics of the transport associated with them extremely relevant to fusion devices.

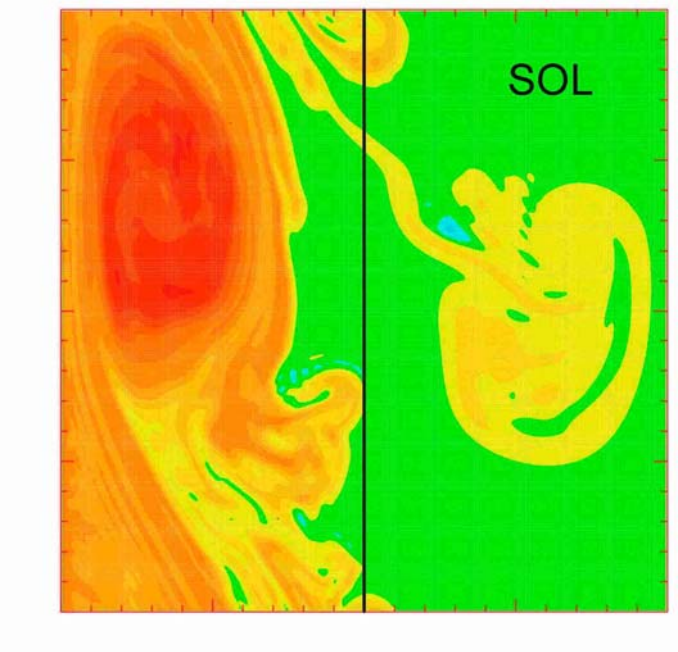

Figure 2. Temperature fluctuations during an eruption.

1. V. Naulin, J. Nycander and J. Juul Rasmussen, Phys. Rev. Lett. **81**, 4148 (1998).

2.4 Ballooning convection: transport modelling beyond slab geometry

O.E. Garcia (also at: Department of Physics, University of Tromsø, Norway),
V. Naulin, A.H. Nielsen and J. Juul Rasmussen
odd.erik.garcia@risoe.dk

A new fluid model of low-frequency fluctuations and convective particle and heat transport in toroidally magnetized plasmas has been derived. It takes into account the full normal and geodesic curvatures of the equilibrium toroidal magnetic field. In the local limit it reduces to the classical model of two-dimensional Rayleigh-Bénard convection. The model readily predicts the experimentally observed ballooning structure of fluctuation amplitudes and radial transport - hence the proposed name. Moreover, due to geodesic curvature there is a new mechanism for generation of differential rotation that accompanies the well-known tilting

instability by inhomogeneous Reynolds stresses. This leads to new dynamical modes termed geodesic oscillations.

Numerical simulations have demonstrated a rich variety of transport states. Close to the dissipative threshold we observe different modes of stationary convection. Further from the threshold different forms of geodesic oscillations are observed and, ultimately, a turbulent state ensues. In numerical simulations we have also for the first time observed a stationary state of suppressed non-linear transport corresponding to a high confinement regime. Figure 3 shows the spatial structure of the pressure, the electrostatic potential and the radial convective heat flux for the stationary high confinement regime, respectively. Note the presence of only closed streamlines that prevents strong non-linear heat transport to the confining outer boundary.

In the near future the model will be improved to conserve the true physical energy integral. This will then be implemented in cylinder coordinates to yield the first numerical solutions with this property that is essential for the prediction of transport suppression and confinement improvement by self-sustained sheared flows.

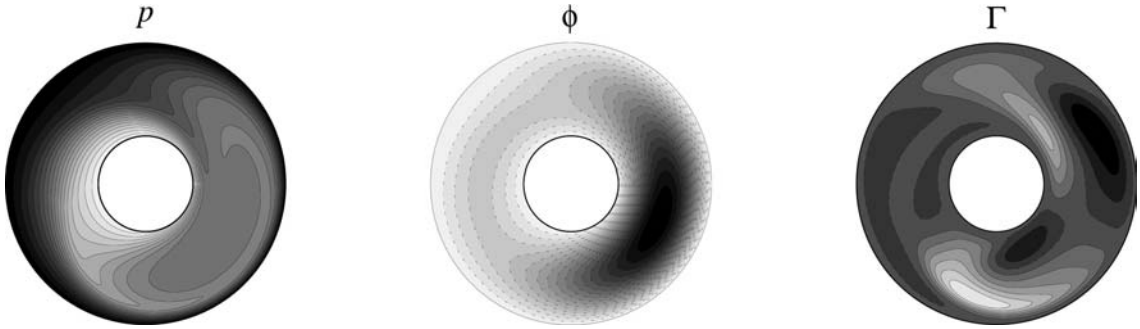

Figure 3. The distribution of pressure p, electrostatic potential φ and radial heat flux Γ in the annulus domain for the Rayleigh number R = 5.0 10^4. Note the presence of only closed streamlines in the potential φ.

2.5 Two-dimensional fluid equations for low-frequency convective modes in a plasma with full density variation

O.E. Garcia (also at Department of Physics, University of Tromsø, Norway),
V. Naulin, A.H. Nielsen and J. Juul Rasmussen
jens.juul.rasmussen@risoe.dk

Cross-field transport is one of the most important and difficult areas of fusion research. Recent experimental observations have revealed that the transport in the edge plasma involves large outbreaks of bursts of density and heat that has a significant effect on the profiles of density and temperature. It is thus obvious that a full description of the edge dynamics *must* include the evolution of the full profiles. A local model or a Boussinesq-like model, where the "background" profile is separated from the fluctuations, as it is standard in dynamical models, cannot describe the essential features.

We have attempted to derive a consistent set of equations describing the low-frequency 2D evolution in a slab geometry that models the outboard mid-plane of a toroidal device. The model, which is based on the fluid equations, governs the two-dimensional dynamics of the interchange convection modes. It describes the fluid drifts accurately in the presence of an inhomogeneous, curved magnetic field. In addition, it describes the adiabatic compression of a fluid parcel that is displaced into a region with a larger magnetic field. The full density

(including profile) is allowed to evolve self-consistently under the influence of an external forcing, and so is the background potential profile, which corresponds to a mean flow. The model will be the basis for a numerical investigation of the dynamics of bursty transport events in the edge plasma.

2.6 3D Drift-Alfvén turbulence

V. Naulin and J. Juul Rasmussen
volker.naulin@risoe.dk

Turbulence in the edge of plasma fusion devices is one of the biggest challenges on the way towards building an efficient, well-controlled fusion power source. Using the TYR code we investigate the interaction between (a) shear flows created by the turbulence and (b) the transport. The TYR code includes the effects of curvature and shear in a geometry following a magnetic flux tube. In addition to the usual E×B fluctuating transport, the fluctuating magnetic field gives rise to radial transport of heat and matter as plasma flows along the perturbed magnetic field. One interesting consequence is that sheared flows can influence these transport components in quite different ways. While flow shear usually suppresses E×B flux, the shear flow is correlated with large current fluctuations. These fluctuations give rise to large magnetic perturbations and, thus, to increased levels of radial plasma transport due to magnetic field perturbations. While this contribution to the total transport is in general rather small, it can enhance the radial flux locally and as a result make the transport reduction due to shear flows less efficient. Large-scale simulations at high resolutions have been performed and they showed the detailed correlations between the fluxes (depicted in Figure 4 and Figure 5) and the correlations between flows and fluxes. The inclusion of temperature fluctuations is in progress.

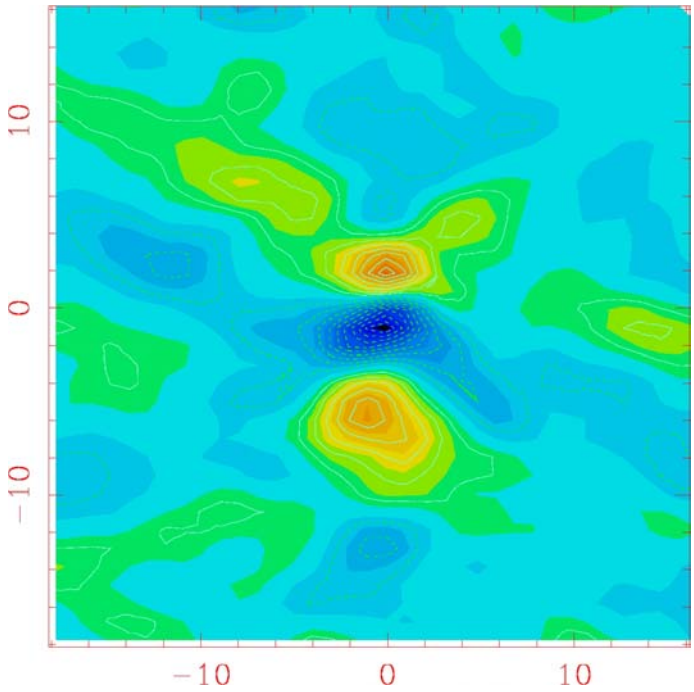

Figure 4. Spatial correlation (radially and poloidally) between ExB and electromagnetic flux, showing a well defined negative correlation for zero offset. Thus, the electromagnetic flux is large where the ExB flux is small.

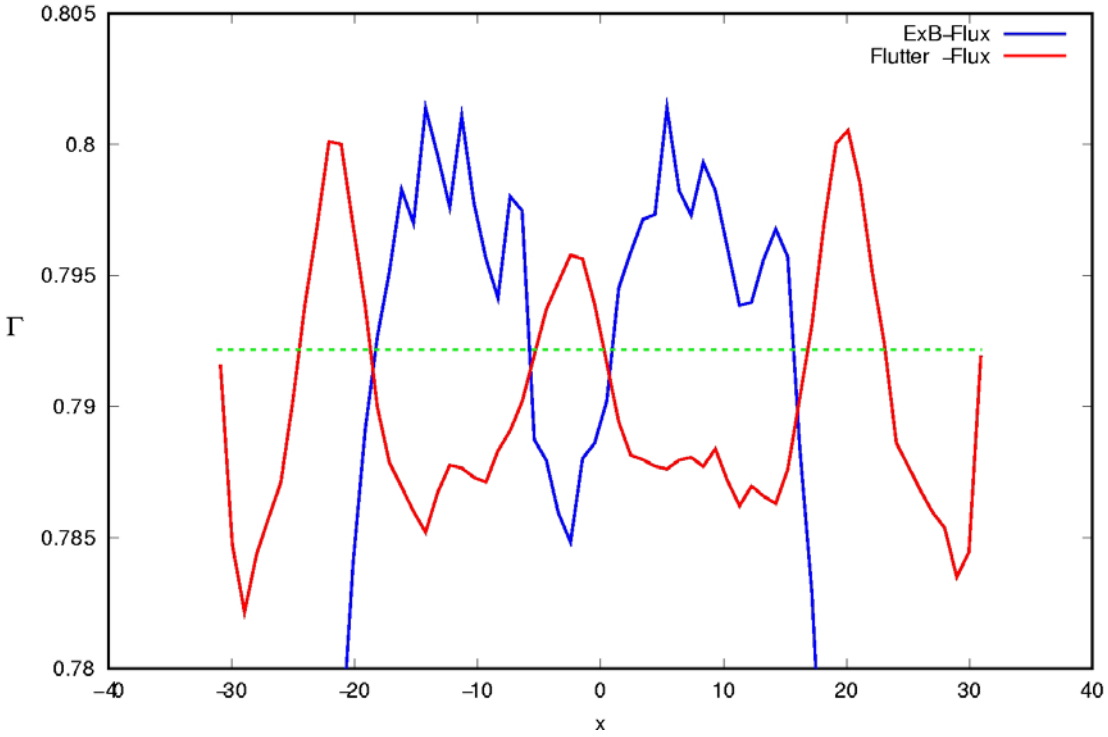

Figure 5. Radial profile of electromagnetic (flutter) flux and E×B transport, showing that both add up to a radially constant value.

2.7 Influence of neutrals on drift and drift Alfvén waves

O. Grulke, Th. Klinger*, Ch. Schroeder* (*IPP Greifswald, Germany) and V. Naulin*
volker.naulin@risoe.dk

In the edge regions of plasmas the concentration of neutrals becomes rather large and the frequency at which the ions collide with the neutrals is no longer negligible. These collisions change the properties of the drift waves, the turbulence and, ultimately, the transport.

Experimental results on drift Alfvén waves indicate insufficient agreement with theoretical predictions that do not include these collisional effects. To be able to compare theory and experiment successfully they therefore have to be accounted for.

For this purpose an eigenmode solver was developed which can use experimental profiles and collision frequencies to calculate the eigenfrequencies and the mode profiles of drift waves. Initial results show that the collisions drastically reduce the wave frequencies. A typical plot of the mode structures for a Gaussian-like density and collision profile is shown in Figure 6.

The results of the linear analysis will be verified against experimental results and results from a full 3D model.

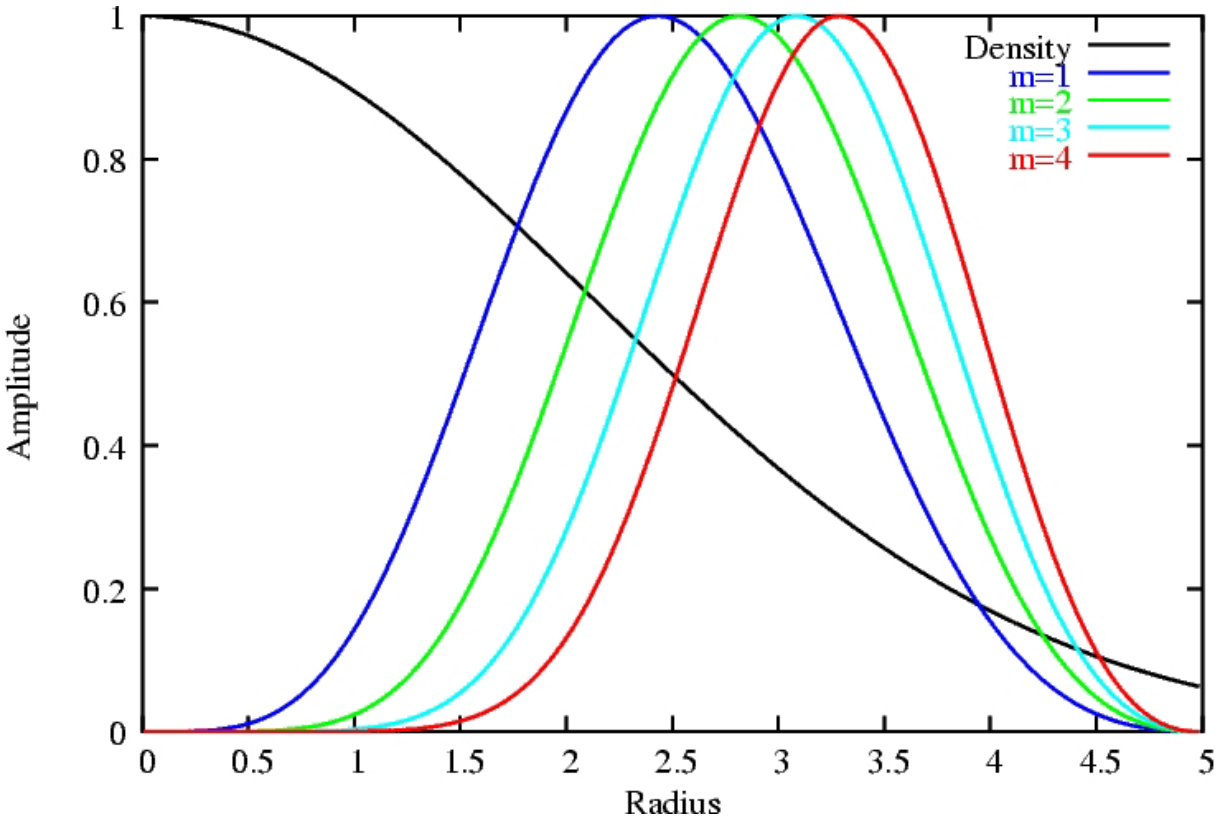

Figure 6: Radial mode structure for drift waves in a cylindrical plasma with radially varying collision frequencies.

2.8 Shear flow generation in 3D drift wave turbulence

S.B. Korsholm, V. Naulin, J. Juul Rasmussen and P.K. Michelsen
soeren.korsholm@risoe.dk

Large-scale poloidal shear flows are expected to be generated spontaneously by drift wave turbulence in magnetized plasmas in toroidal devices. These flows may regulate the turbulence by suppressing the small-scale structures and set up transport barriers which can induce a transition from low (L-mode) to high (H-mode) confinement. We have investigated the generation of shear flows by drift wave turbulence using numerical solutions of the three-dimensional Hasegawa-Wakatani (HW) equations. The simulations are performed in a slab geometry periodic in y (poloidal direction) and z (toroidal direction) and bounded in the radial direction, x, by non-permeable walls. In this part of the work we have been particularly interested in investigating the cause of the shear flow generation. While it is clear that the Reynolds stress (Re) is responsible for generating the poloidal flow, it is not clear which modes contribute mostly to Re. The HW-model contains both the drift wave component with finite parallel wave number, k_z, and the flute mode (convective cell) component having $k_z = 0$. The drift modes are linearly unstable and grow until they reach a non-linear level, where they couple to the flute modes.

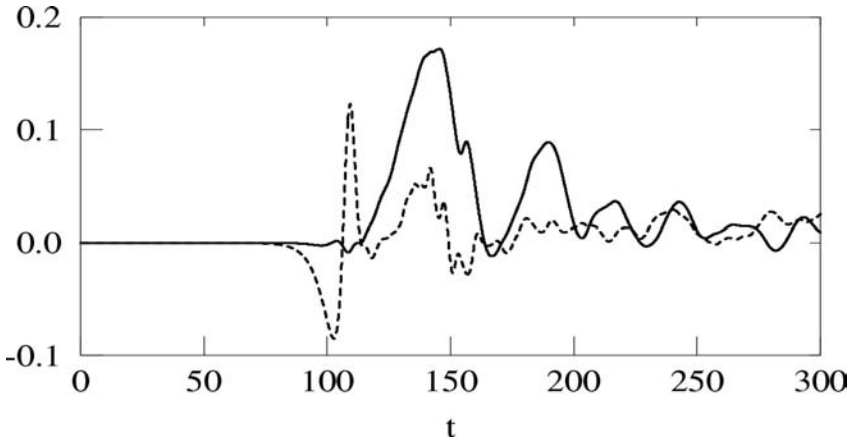

Figure 7. The temporal evolution of the contributions to the Reynolds stress from the flute mode (full line) and the drift mode (dashed line).

In Figure 7 we show the temporal evolution of the separate contributions to Re from the drift and the flute modes, respectively. We observe that initially Re is driven by the drift wave component, but when the poloidal flow (characterized by $k_y = k_z = 0$) has been established, the main contribution to Re originates from the flute modes. Ultimately, when the system has settled into a quiescent state, the two contributions become comparable and small. This implies that Re is in part driven by a non-linear instability, i.e. the flow is self-amplifying from the seed produced by the drift modes. These results emphasize the importance of considering both the direct contribution to Re by the drift modes and the contribution via the flute modes. The latter contribution is usually not accounted for in theoretical descriptions of the shear flow generation based on the simplified Hasegawa-Mima type models.

2.9 Modelling the formation of large-scale zonal flows in drift wave turbulence in a rotating fluid experiment

V. Naulin, J. Juul Rasmussen, B. Stenum, L.J.A. van Bokhoven (University of Eindhoven, Eindhoven, the Netherlands) and J. van de Konijnenberg
jens.juul.rasmussen@risoe.dk

The self-consistent generation of large-scale flows - zonal flows - by the rectification of small-scale turbulent fluctuations is of great importance both in geophysical flows and in magnetically confined plasmas. These flows can regulate the turbulence by suppressing the small-scale structures. Eventually the flows act to set up transport barriers. A relatively pedagogical description of the generation of zonal flows is provided by the idea of homogenisation of the so-called potential vorticity, which is a Lagrangian invariant of the flow, relying on the mixing properties of the turbulence.

We have modelled the generation of zonal flows by drift wave turbulence in a magnetized plasma by exploiting the analogy between Rossby wave dynamics on the β-plane and drift-wave dynamics in a magnetized plasma with a density gradient perpendicular to the magnetic field. Corresponding laboratory experiments in a rotating fluid were performed to investigate the formation of large-scale flows by mixing and homogenisation of the potential vorticity.

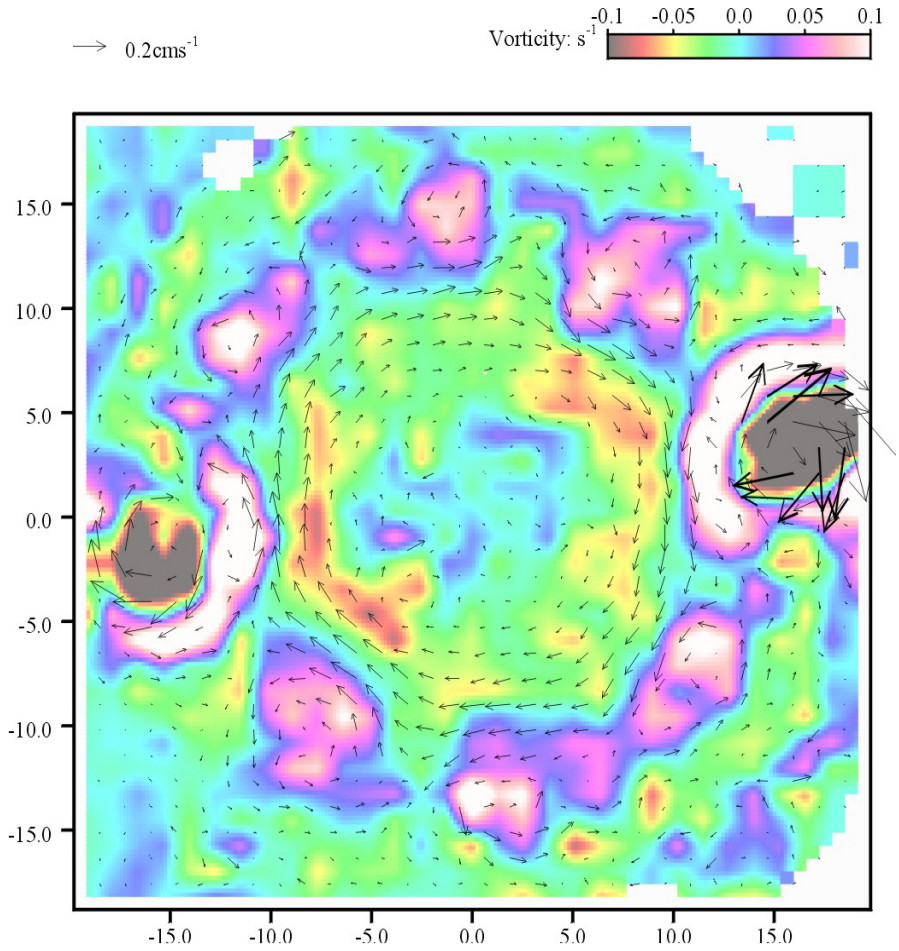

Figure 8. Velocity field shown by arrows and vorticity contours averaged over 10 forcing periods. The scales for the fields are indicated above the figure.

The experiments are conducted in a tank with radially symmetric bottom topography and a rigid lid. The bottom has a constant negative slope, β, in the radial direction. For this system the so-called potential vorticity PV = ω + βr is a Lagrangian conserved quantity. Here ω is the relative vorticity. Thus, it is readily seen that an effective mixing that homogenises PV will lead to replacing the high PV near the centre with low PV from the outside, and this will appear as an anticyclonic vortex over the centre. In the experiment the mixing is forced by periodical pumping near the outer boundary of the tank, and the azimuthally averaged forcing is zero. The velocity field is measured by particle tracking in the horizontal plane. After a transient time of several tens of forcing periods, we observe the formation of a zonal velocity in the anti-cyclonic direction. This is illustrated in Figure 8, where we show the velocity and the vorticity field obtained several tens of periods after the forcing was started. The fields have been averaged over 10 forcing periods. The zonal velocity peaks in the region away from the forcing regime, see Figure 9, which depicts the velocity field of Figure 8 averaged over the azimuthal direction to obtain the zonal velocity. These observations are in agreement with the discussion above. As a control case, we checked that no zonal flow appeared in the case of a flat bottom.

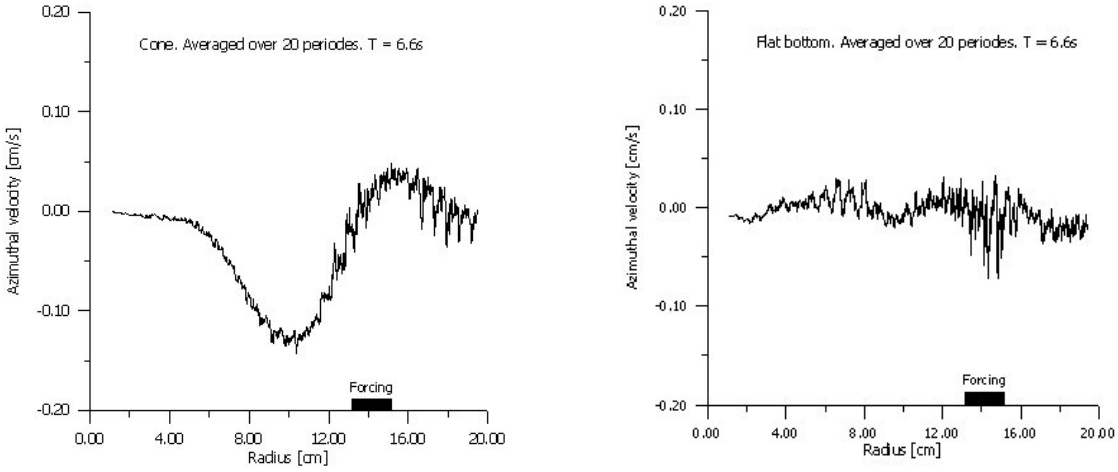

Figure 9. Averaged azimuthal velocity versus radius. The left frame shows the velocity for the case of the cone-shaped bottom, while the right frame shows the reference case with a flat bottom. The black bar shows the position of the forcing region.

The experimental results are supported by direct numerical solutions of the quasi-geostrophic vorticity equation in the β-plane approximation that models the experimental situation. This model equation is equivalent to the Hasegawa-Mima equation that describes drift wave dynamics in magnetized plasma. The mechanism of the formation of zonal flows by drift wave turbulence is just equivalent to the one in the fluid experiment. This indicates that zonal flows are the natural structures apparent in drift-wave type turbulence, while transport enhancing "streamers", flow structures along the gradient, are of a more "artificial" nature.

2.10 Development of collective Thomson scattering for diagnosing fast ion dynamics

H. Bindslev, S. Korsholm, P. Michelsen, E. Tsakadze, M. Jessen, J. Holm, S. Nimb, B. Sass, J. Thorsen, P. Woskov (MIT, Cambridge, USA), TEC team (FZ-Jülich, Germany; FOM-Rijnhuizen, Netherlands; ERM/KMS, Belgium), ASDEX upgrade team (Max Planck Institut fürPlasmaphysik, Garching, Germany)
henrik.bindslev@risoe.dk; www.risoe.dk/euratom/cts

Magnetically confined fusion plasmas contain highly non-thermal populations of fast ions resulting from fusion reactions and plasma heating. With energies in the MeV range, two to three orders of magnitude above the bulk ion and electron energies, the fast ions typically carry 1/3 of the plasma kinetic energy and even more of the free energy. It is essential that these energetic ions remain confined while they slow down and heat the thermal bulk plasma. The free energy associated with the fast ions is, however, also available for mischief. Non-linear wave particle interaction can drive waves and turbulence in the bulk plasma, significantly affecting both bulk and fast ion dynamics. In particular, it can lead to catastrophic loss of fast ion confinement. The sawtooth instability, also affected by fast ions, appears to redistribute part of the ion population. If properly tailored, this can be an effective tool for removing helium ash from the core while leaving the valuable energetic alpha particles in place.

Wave particle interaction is also the basis of ion cyclotron resonance heating (ICRH), one of the main plasma heating schemes relying on the absorption of radio waves. Wave particle interaction depends critically on the phase space distribution of the energetic ions. The effect of waves and turbulence on the ion population manifests itself in the phase space distribution. So both to challenge and guide our understanding of dynamics involving fast ions, and to monitor our attempts at tailoring turbulence and instabilities affecting the ions, we need detailed measurements of the ion phase space distribution.

It has long been realized that collective Thomson scattering (CTS) has a unique capability for diagnosing the ion phase space distribution; that is, it can provide spatially resolved measurements of the velocity distribution. There are other techniques for diagnosing fast ions (charge exchange neutral particle spectroscopy and neutron spectroscopy), but no other diagnostic currently holds the potential for simultaneously resolving the distributions in time, space and velocity. Building on the experience gained with the fast ion CTS diagnostic at JET,[0] the technique had its breakthrough at TEXTOR Tokamak in Forshungszentrum Jülich, Germany, where a TEC-MIT team led by H. Bindslev built a proof-of-principle experiment.[2] This experiment demonstrated the feasibility of the measurements[3] and provided a wealth of new data on spatially localized ion velocity distributions at many time points in each plasma shot. These have, among others, permitted the investigation of fast ion dynamics at saw teeth.

In 2002 a team[4] of four physicists and five technicians was collected at Risø to continue developing and exploiting fast ion CTS in close collaboration with MIT,[5] The Max Planck Institute for Plasma Physics[6] and the Trilateral Eurogio Cluster (TEC).[7] This year activities in the newly formed CTS team at Risø focussed on developing a significant upgrade to the TEXTOR fast ion CTS system, and designing a new fast ion CTS system to ASDEX Upgrade Tokamak at the Max Planck Institute for Plasma Physics in Garching, Germany.[8] The work on the TEXTOR system includes the development of a new motor steerable antenna, a new transmission line and a universal polariser, significant upgrades to the receiver electronics and a new data acquisition system. For the ASDEX system activities included design and procurement. Preferential support from EURATOM was received for the procurement of the system for ASDEX.

To assist in the construction and verification of antennae and transmission lines a rig for measuring radiation patterns was built and operated. With the assistance of international colleagues (direct collaborators mentioned above and additionally colleagues from Institute für Plasmaforschung, University of Stuttgart[9]) these activities have brought a range of new competences to Risø so that the full range of competences for design, construction and testing of the CTS receivers are now in house.

1. H. Bindslev, J. A. Hoekzema, J. Egedal, J. A. Fessey, T. P. Hughes, and J. S. Machuzak, *Phys. Rev. Lett.* **83**, 3206 (1999).
2. H. Bindslev, L. Porte, A. Hoekzema, J. Machuzak, P. Woskov, D. van Eester, 26th EPS Conf. Contr. Fusion and Plasma Physics, Maastricht, Netherlands, Vol. 23J, part II, p765, EPS (1999) (http://epsppd.epfl.ch/Maas/web/pdf/p2049.pdf); H. Bindslev, L. Porte, A. Hoekzema, J. Machuzak, P. Woskov, D. van Eester, J. Egedal, J. Fessey, T. Hughes, *Fusion Engineering and Design*, **53**, 105 (2001); H. Bindslev, Journal of Plasma and Fusion Research. 76, 878 (2000); L. Porte, H. Bindslev, F. Hoekzema, J. Machuzak, P. Woskov, and D. Van Eester, *Rev. Sci. Instrum*. **72**, 1148 (2001); (http://www.risoe.dk/euratom/cts/TEXTOR).
3. H. Bindslev, L. Porte, J. A. Hoekzema, D. Van Eester, A. Messiaen, G. Van Wassenhove and P. Woskov, Proceedings of the 28th EPS conference on Controlled Fusion and Plasma Physics, Madeira 18-22 June 2001. (Or.09 & P3.077) http://www.cfn.ist.utl.pt/EPS2001/fin/pdf/P3.077.pdf;
4. www.risoe.dk/euratom/cts;

5. www.psfc.mit.edu/
6. www.ipp.mpg.de/
7. www.fz-juelich.de/ipp/; www.rijnh.nl; http://fusion.rma.ac.be/
8. www.ipp.mpg.de/eng/for/projekte/asdex/for_proj_asdex.html
9. www.uni-stuttgart.de/ipf/

2.11 Antenna and quasi-optical transmission lines for CTS systems

E. Tsakadze, S. Nimb and B. Sass
erekle.tsakadze@risoe.dk

A new quasi-optical receiver antenna for the collective Thomson scattering (CTS) diagnostic system at the TEXTOR tokamak Jülich, Germany, is being constructed. The transmission line of the antenna includes ellipsoidal and hyperboloidal mirrors. The shapes of the mirrors were calculated using newly developed MATLAB codes that permit transmission lines to be specified by variable sets of constraints. The MATLAB results on mirror and beam shapes were transferred electronically to CAD software, CATIA, for further engineering design such as support and integration with actuators. From CATIA the designed components such as curved mirrors were transferred electronically to CAM software running the CNC cutting tools in the Risø workshop. Figure 1 illustrates the process *from MATLAB to metal* in the case of an ellipsoidal mirror. It should be noted that the duration of whole procedure of the mirror production (from MATLAB to metal) is about 4-5 hours. After the cut, the surfaces of the mirrors are characterized by the surface analyser at Risø's workshop.

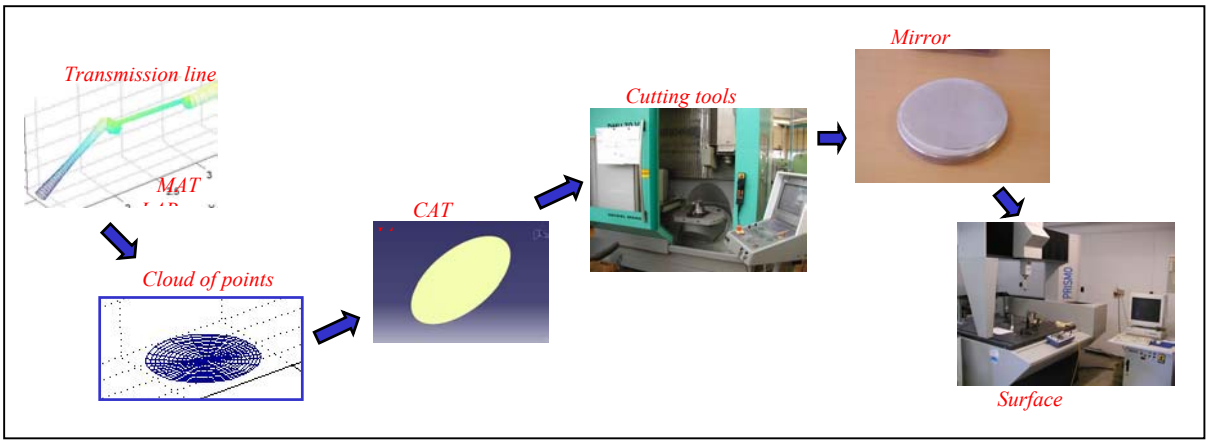

Figure 10. Illustration of the steps in the production of a quazi-optical mirror, from MATLAB to metal.

A similar quasi-optical transmission line is going to be constructed and installed at the ASDEX Upgrade tokamak in Garching, Germany.

1. "Fast ion millimeter wave CTS diagnostics on TEXTOR and ASDEX", S. B. Korsholm, H. Bindslev, J. Egedal, J. A. Hoekzema, F. Leuterer, P. K. Michelsen, E. Tsakadze and P. Woskov, 44th Annual Meeting of the Division of Plasma Physics, American Physical Society (DPP-APS), Orlando, Florida, USA (2002). Bulletin of American Physical Society (APS), p. 84, vol. 47, No. 9, November, 2002.

2.12 Electron cyclotron resonance heating and current drive

H. Bindslev and P. Michelsen
henrik.bindslev@risoe.dk

In magnetically confined toroidal fusion plasmas the electrons gyrate in the confining magnetic field. With field strengths in the range of 2 to 5 tesla, the electron cyclotron frequency is in the range of 56 to 140 GHz. Electromagnetic waves can be absorbed by the electrons at their gyration frequency and at higher harmonics. The radial inhomogeneity of the field gives rise to radial variation in the cyclotron frequency. With electron energies in the range of 10 keV, relativistic Doppler shifts of the cyclotron frequencies are significant. The result is a finite radial extent of the resonance region for absorption of waves with a given frequency. The location of the resonance region moves inwards towards higher fields with increasing frequency, and outwards with decreasing angle between wave vector and magnetic field due to Doppler shifts. The microwaves can propagate in beams with diameters down to a few centimetres, which combined with similar radial dimensions of the resonance region permits localization of the absorption to a very small fraction of the plasma volume. Microwave powers in the range of 1 MW in pulses of 10 or more seconds are provided reliably by gyrotrons.

Electron cyclotron waves (or ECW as microwaves in the electron cyclotron frequency range are often called in the fusion community) are a powerful tool for manipulating plasmas through their capability of providing localized heating and current drive. The objectives of ECW systems include current drive for long pulse operation and current profile manipulation for reversed or low shear operation, central heating to study regimes with dominant electron heating, neo-classical tearing mode (NTM) stabilisation, and tailoring of sawtooth amplitudes and periods. Risø participates in the international effort to design an ECW system for the ITER.

2.13 Operations space diagram for electron cyclotron wave systems

H. Bindslev
henrik.bindslev@risoe.dk

The objectives of electron cyclotron wave (ECW) systems are diverse. Each objective is best met with a particular optimisation of the ECW system. We take optimisation to mean not just how effectively an objective can be accomplished for one set of plasma parameters, but also over how wide a range of plasma parameters (operational range) it can be done.

Optimising the ECW system(s) requires weighting of the objectives and associated operational ranges from which a compromise can be found. This process was pursued in the design of the now disbanded ECW system for JET, and was carried out for ITER. The design optimisation includes choice of frequency or frequencies, launch locations and steering ranges of the ECW beams. Documenting the capabilities at various frequencies and launcher locations readily leads to a plethora of plots and tables that obscure the overview. In the study for the JET-ECW system a wealth of computations were presented. To gain the overview required to strike a suitable compromise between disparate objectives, it was useful to present the computed performance estimates in low-dimensional parameter spaces, focusing on those

parameters that yield the largest variants of system performance. Such a space was identified. It leads to a presentation of the operational possibilities in a Clemmov-Mullaly-Allis (CMA) type diagram, the ECW-CMA diagram, see Figure 11. In this diagram, with normalized density and normalized field coordinates, the parameter range in which it is possible to achieve a given task (e.g. O-mode current drive for stabilising a neoclassical tearing mode) appears as a region. With also the Greenwald density limit shown, this diagram condenses the information on operational possibilities, facilitating the overview required at the design phase. At the operations phase it may also prove useful in setting up experimental scenarios by showing operational possibilities, avoiding the need for survey-type ray tracing at the initial planning stages. The diagram may also serve the purpose of communicating operational possibilities to non-experts. This work was presented at the 12th Joint Workshop on Electron Cyclotron Emission and Electron Cyclotron Resonance Heating.[1]

1. H Bindslev, "*Operations Space Diagram for ECRH and ECCD in JET and ITER*", 12th Joint Workshop on Electron Cyclotron Emission and Electron Cyclotron Resonance Heating, Aix-en-Provence, France, May 13-16, 2002.

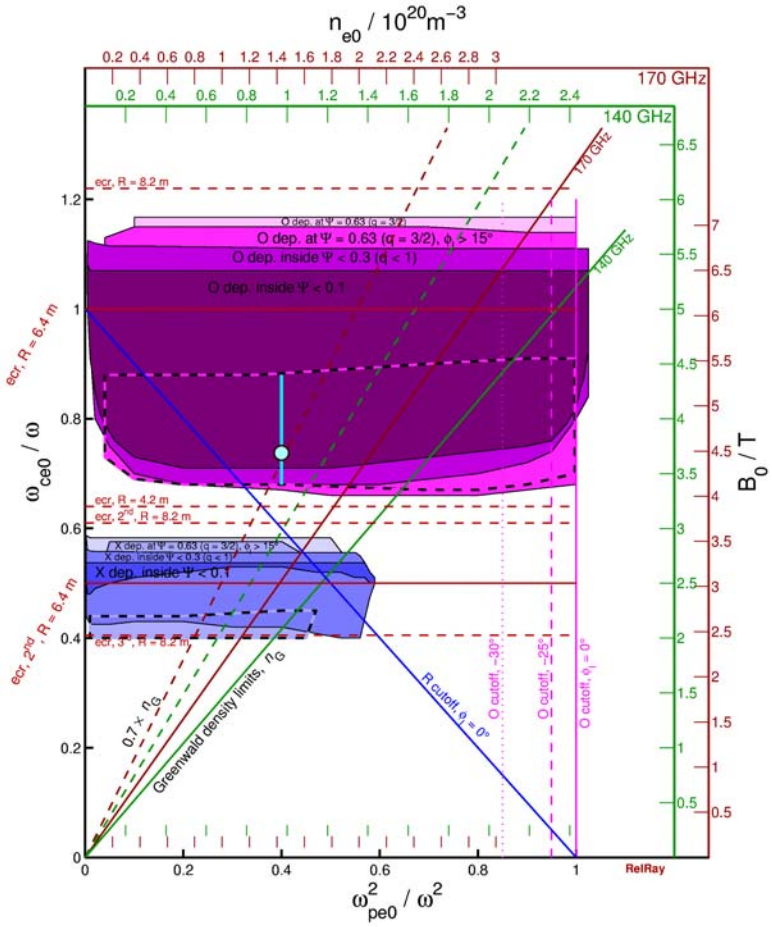

Figure 11. ECW-CMA diagram indicating operational ranges for an ITER ECW system. The axes bottom and left are normalized central density and magnetic fields. Axes top and right have physical units for a selection of EC wave frequencies. The coloured patches indicate operational ranges where deposition within a given flux surface can be achieved with O-mode and X-mode, respectively. Parameters at which EC waves are cut off at the centre are shown, as are the locations of various cyclotron resonances. The locations of the Greenwald density limits have been plotted for a selection of frequencies.

2.14 Position control of electron cyclotron resonance heating launcher mirrors by laser speckle sensor

R. Skov Hansen, P. K. Michelsen, S. G. Hanson and H. Bindslev
poul.michelsen@risoe.dk

Electron cyclotron resonance heating, ECRH, systems are important for localised plasma heating in present and future plasma devices as, e.g., ITER. In order to have high reproducibility of the ECRH beam direction, it is necessary to know and control the exact positions of the mirrors that direct the microwave beam towards the plasma. This is not a trivial problem because of (a) thermal expansion of the vessel structures, the launcher itself and its support structure, (b) the mechanical load on the mirrors and the support structures and (c) the accessibility to the various mirrors. We suggest the use of a new technique published recently[1] that is based on a non-contact laser speckle sensor for measuring one- and two-dimensional angular displacement. The method is based on Fourier transforming the scattered field from a single laser beam that illuminates the target, here assumed to be rough and not giving rise to specular reflection. The angular distribution of the light field at the target is linearly mapped onto an image sensor array placed in the Fourier plane. Measuring the displacement of this so-called speckle pattern facilitates the determination of the mirror orientation. If a laser beam illuminates the diffuse backside of the mirror, and the speckle pattern is monitored by a detector (a CCD camera or similar), very small angular displacement can be detected.

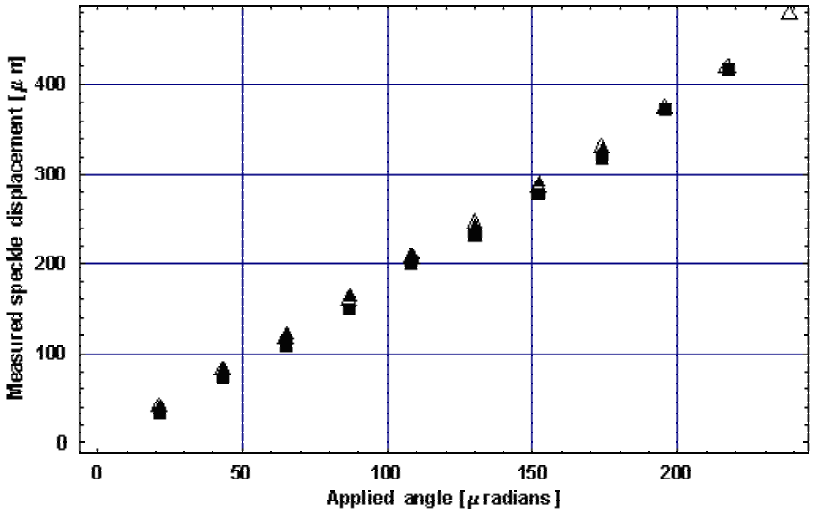

Figure 12 Correspondence between applied values of the angular displacements and the corresponding displacements of the speckle pattern. The triangles represent measurements performed at the centre of rotation and the squares represent measurements performed 70 mm from the axis of rotation.

A series of experiments were performed by probing a diffuse target that was angularly displaced by piezo-electrical tilting of a thin plane target across a knife edge. Corresponding readings of applied values for the angular displacement and measured displacement of the speckle pattern are presented in Figure 12 where the measuring distance was four meters. This

demonstrates that the technique can been extended to long measuring distances. The obtained angular resolution of the order of a few μrad is in agreement with theoretical predictions. This work was presented at the 12th Joint Workshop on Electron Cyclotron Emission and Electron Cyclotron Resonance Heating.[2]

1. B. Rose, H. Imam and S. G. Hanson, "Non-contact laser speckle sensor for measuring one- and two-dimensional angular displacement," *J. Opt.* **29**, 115-120 (1998).
2. H. Bindslev, S. G. Hanson and **P. K. Michelsen,** "Position control of ECRH launcher mirrors by laser speckle sensor and infrared spot detection", 12th Joint Workshop on Electron Cyclotron Emission and Electron Cyclotron Resonance Heating, Aix-en-Provence, France, May 13-16, 2002.

2.15 Publications and conference contributions

2.15.1 International publications

Akers, R.J.; Counsell, G.F.; Sykes, A.; Appel, L.C.; Arends, E.R.; Byrom, C.; Carolan, P.G.; Conway, N.J.; Cunningham, G.; Dnestrovskij, A.; Dnestrovskij, Y.N.; Field, A.R.; Fielding, S.J.; Gryaznevich, M.; Helander, P.; Kirk, A.; Korsholm, S.B.; Martin, R.; Meyer, H.; Nightingale, M.P.S.; Roach, C.M.; Shevchenko, V.; Tournianski, M.; Walsh, M.J.; Warrick, C.D., L-H transition in the mega-Amp spherical tokamak. Phys. Rev. Lett. (2002) v. 88 p. 035002.1-035002.4

Basse, N.P.; Michelsen, P.K.; Zoletnik, S.; Saffman, M.; Endler, M.; Hirsch, M., Spatial distribution of turbulence in the Wendelstein 7-AS stellarator (invited paper). Plasma Sources Sci. Technol. (2002) v. 11 (no.3A) p. A138-A142

Basse, N.P.; Zoletnik, S.; Saffman, M.; Baldzuhn, M.; Endler, M.; Hirsch, M.; Knauer, J.P.; Kühner, G.; McCormick, K.; Werner, A., Low- and high-mode separation of short wavelength turbulence in dithering Wendelstein 7-AS plasmas. Phys. Plasmas (2002) v. 9 p. 3035-3049

Benilov, E.S.; Naulin, V.; Juul Rasmussen, J., Does a sheared flow stabilize inversely stratified fluid?. Phys. Fluids (2002) v. 14 p. 1674-1680

Juul Rasmussen, J.; Nielsen, A.H.; Naulin, V., Dynamics of vortex interactions in two-dimensional flows. Physica Scripta (2002) v. T98 p. 29-33

Naulin, V., Aspects of flow generation and saturation in drift-wave turbulence. New J. Phys. (2002) v. 4 p. 28.1-28.18

Ribeiro, C.; Akers, R.; Alladio, F.; Axon, K.; Baylor, L.; Counsell, G.F.; Dowling, J.; Fielding, S.; Garzotti, L.; Gryaznevich, M.; Han, W.E.; Innocente, P.; Jenkins, I.; deKloe, J.; Martin, R.; Micozzi, P.; Sass, B.; Sykes, A.; Terranova, D., Todd, T.N.; Twynam, P.; Wakatani, M.; Walsh, M.J.; You, S., Pellet injection on START and MAST. Fusion Eng. Des. (2001) v. 58/59 p. 319-324

Ruban, V.P., Current-sheet formation in incompressible electron magnetohydrodynamics. Phys. Rev. E (2002) v. 65 p. 047401.1-047401.4

Zoletnik, S.; Basse, N.P.; Saffman, M.; Svendsen, W.; Endler, M.; Hirsch, M.; Werner, A.; Fuchs, C., Changes in density fluctuations associated with confinement transitions close to a rational edge rotational transform in the W7-AS stellarator. Plasma Phys. Control. Fusion (2002) v. 44 p. 1581-1607

2.15.2 Danish publications

Basse, N.P., Turbulence in Wendelstein 7-AS plasmas measured by collective light scattering. Risø-R-1355(EN) (2002) 166 p. (ph.d. thesis) www.risoe.dk/rispubl/ofd/ris-r-1355.htm

Bindslev, H.; Singh, B.N (eds.), Association Euratom - Risø National Laboratory annual progress report 2001. Risø-R-1345(EN) (2002) 49 p. www.risoe.dk/rispubl/ofd/ris-r-1345.htm

Dannemand Andersen, P.; Michelsen, P.K., Emerging energy technologies. In: Larsen, H.; Sønderberg Petersen, L. (eds.), Risø National Laboratory (DK). Systems Analysis Department. Risø energy report 1. New and emerging technologies - options for the future. Risø-R-1351(EN) (2002) p. 19-22 www.risoe.dk/rispubl/SYS/ris-r-1351.htm

Lynov, J.-P., Fusion energy. In: Larsen, H.; Sønderberg Petersen, L. (eds.), Risø National Laboratory (DK). Systems Analysis Department. Risø energy report 1. New and emerging technologies - options for the future. Risø-R-1351(EN) (2002) p. 50-52 www.risoe.dk/rispubl/SYS/ris-r-1351.htm

2.15.3 Conference lectures

Basse, N.P.; Zoletnik, S.; Saffman, M.; Endler, M.; Hirsch, M., Separation of L- and H-mode density fluctuations in dithering Wendelstein 7-AS plasmas (poster). In: Proceedings. 28. European Physical Society conference on controlled fusion and plasma physics, Funchal (PT), 18-22 Jun 2001. Silva, C.; Varandas, C.; Campbell, D. (eds.), (Instituto Superior Tecnico, Lisboa, 2001) (Europhysics Conference Abstracts, vol. 25A) p. 1941-1944 www.cfn.ist.utl.pt/EPS2001/fin/authors/nav/AutS01fr.html

Bindslev, H.; Porte, L.; Hoekzema, J.A.; Woskov, P.; Eester, D. Van; Messiaen, A.; Wassenhove, G. Van, Fast ion dynamics in TEXTOR measured by collective Thomson scattering (oral presentation). In: Proceedings. 28. European Physical Society conference on controlled fusion and plasma physics, Funchal (PT), 18-22 Jun 2001. Silva, C.; Varandas, C.; Campbell, D. (eds.), (Instituto Superior Tecnico, Lisboa, 2001) (Europhysics Conference Abstracts, vol. 25A) p. 453-456 www.cfn.ist.utl.pt/EPS2001/fin/authors/nav/AutB03fr.html

Bindslev, H.; Porte, L.; Hokzema, J.A.; Woskov, P., Fast ion dynamics measured by collective Thomson scattering of MM waves. In: Proceedings. 10. International symposium on laser-aided plasma diagnostics (LAPD-10), Fukuoka (JP), 24-28 Sep 2001. Muraoka, K. (ed.), (Kyushu University, Kyushu, 2002) p. 97-108

Bindslev, H.; Porte, L.; Hokzema, J.A.; Woskov, P.; Eester, D. Van, Fast ion dynamics measured by collective Thomson scattering. In: Advanced diagnostics for magnetic and inertial fusion. Proceedings. International conference on advanced diagnostics for magnetic and inertial fusion, Varenna (IT), 3-7 Sep 2001. Stott, P.E.; Wootton, A.; Gorini, G.; Sindoni, E.; Batani, D. (eds.), (Kluwer Academic, New York, 2002) p. 311-318

Juul Rasmussen, J.; Naulin, V.; Nielsen, A.H.; Nycander, J., Transport barriers and ELMs in flute mode turbulence (poster). In: Contributed papers on CD-ROM. 29. European Physical Society conference on plasma physics and controlled fusion, Montreux (CH), 17-20 Jun 2002. Behn, R.; Varandas, C. (eds.), (European Physical Society, Paris, 2002) (Europhysics Conference Abstracts 26 B) 4 p. (P-3.217)

Korsholm, S.B.; Michelsen, P.K.; Naulin, V.; Juul Rasmussen, J., Analysis of determination of Reynolds stress in drift wave turbulence (poster). In: Proceedings. 28. European Physical Society conference on controlled fusion and plasma physics, Funchal (PT), 18-22 Jun 2001. Silva, C.; Varandas, C.; Campbell, D. (eds.), (Instituto Superior Tecnico, Lisboa, 2001) (Europhysics Conference Abstracts, vol. 25A) p. 2133-2136 www.cfn.ist.utl.pt/EPS2001/fin/authors/nav/AutN01fr.html

Naulin, V.; Schröder, C.; Klinger, T.; Blick, D.; Piel, A.; Bonhomme, G.; Korsholm, S.B., Taming driftwave turbulence: Numerical simulations and experiment (poster). In: Proceedings. 28. European Physical Society conference on controlled fusion and plasma physics, Funchal (PT), 18-22 Jun 2001. Silva, C.; Varandas, C.; Campbell, D. (eds.), (Instituto Superior Tecnico, Lisboa, 2001) (Europhysics Conference Abstracts, vol. 25A) p. 1713-1716 www.cfn.ist.utl.pt/EPS2001/fin/authors/nav/AutN01fr.html

Nielsen, A.H.; Naulin, V.; Juul Rasmussen, J., Two-dimensional turbulence on bounded domains. In: Advances in turbulence IX. Proceedings. 9. European turbulence conference, Southampton (GB), 2-5 Jul 2002. Castro, I.P.; Hancock, P.E.; Thomas, T.G.; (eds.), (International Center for Numerical Methods in Engineering, Barcelona, 2002) p. 767-770

Porte, L.; Bindslev, H.; Hoekzema, F.; Korsholm, S.B.; Kruyt, O.G.; Prins, R.; Woskov, P., Fast-ion collective Thomson scattering diagnostic on TEXTOR Tokamak (poster). In: Proceedings. 28. European Physical Society conference on controlled fusion and plasma physics, Funchal (PT), 18-22 Jun 2001. Silva, C.; Varandas, C.; Campbell, D. (eds.), (Instituto Superior Tecnico, Lisboa, 2001) (Europhysics Conference Abstracts, vol. 25A) p. 425-428 www.cfn.ist.utl.pt/EPS2001/fin/sessions/nav/Poster18fr.html

2.15.4 Publications for a broader readership

Jensen, V.O., Fusionsenergi - fremtidens energikilde?. *Aktuel Naturvidenskab* (2002) (no.1) p. 11-14

Jensen, V.O., Fusionsenergi. Fremtidens dominerende energikilde?. (Fysikforlaget, København, 2002) (elektronisk) 65 p. www.fy.gymfag.dk/

2.15.5 Unpublished Danish lectures

Bindslev. H., Fusion, en universel energikilde. Forelæsning på Øregård Gymnasium, Gentofte (DK), 1 Oct 2002. Unpublished.

Jensen, V.O., Uendelig energi - fremtidens energi. Dansk Naturvidenskabsfestival 2002. Næstved Tekniske Gymnasium, Næstved (DK), 25 Oct 2002. Unpublished.

Michelsen, P.K., Fusionsenergi - er det en mulighed. Foredrag på DTU for elever fra HTX i Herning, Lyngby (DK), 3 Oct 2002. Unpublished.

Michelsen, P.K., Fusionsenergi - er det en mulighed?. Møde i Naturvidenskabeligt Selskab på Fyn, Odense (DK), 20 Nov 2002. Unpublished.

Michelsen, P.K., Kursus i plasmafysik (kursus 10477). Forelæsningsrække på Danmarks Tekniske Universitet (26 forskellige forelæsninger), Lyngby (DK), 4 Sep - 4 Dec 2002. Unpublished. Michelsen, P.K., Uendelig energi - fremtidens energi. Forelæsning på Fredericia-Middelfart Tekniske Gymnasium, Middelfart (DK), 2 Oct 2002. Unpublished.

2.15.6 Unpublished international lectures

Basse, N.P., Turbulence in high-density H-mode plasmas. In: Abstracts. Workshop on turbulence and anomalous transport in plasmas and fluids, Risø (DK), 6-8 May 2002. (Risø National Laboratory, Roskilde, 2002) 1 p.

Basu, R., Particle dynamics in the Hasegawa-Wakatani model. In: Abstracts. Workshop on turbulence and anomalous transport in plasmas and fluids, Risø (DK), 6-8 May 2002. (Risø National Laboratory, Roskilde, 2002) 1 p.

Bindslev, H., Fast ion dynamics measured by collective Thomson scattering (invited lecture). German-Polish EURO-conference on plasma diagnostics for fusion and applications, Greifswald (DE), 4-6 Sep 2002. Unpublished.

Bindslev, H., Fast ion dynamics measured by collective Thomson scattering. Lecture at Institut für Plasmaforschung, Stuttgart University, Stuttgart (DE), 6 Jun 2002. Unpublished.

Bindslev, H.; Porte, L.; Hoekzema, J.A.; Woskov, P., Fast ion dynamics measured by collective Thomson scattering (invited oral presentation). 14. Annual topical conference on high temperature plasma diagnostics, Madison, WI (US), 8-11 Jul 2002. Unpublished.

Bindslev. H., Operations space diagram for ECRH and ECCD in JET and ITER (poster). In: Book of abstracts. 12. Joint workshop on electron cyclotron emission and electron cyclotron resonance heating, Aix-en-Provence (FR), 13-16 May 2002. (Conference Committee, Aix-en-Provence, 2002) p. 35

Bindslev. H.; Hanson, S.G.; Michelsen, P.K., Position control of ECRH launcher mirrors by laser speckle sensor and infrared spot detection (poster). In: Book of abstracts. 12. Joint workshop on electron cyclotron emission and electron cyclotron resonance heating, Aix-en-Provence (FR), 13-16 May 2002. (Conference Committee, Aix-en-Provence, 2002) p. 97

Juul Rasmussen, J.; Naulin, V.; Stenum, B.; Bokhoven, L.J.A. van; Konijnenberg, J. van de, Modelling the formation of zonal flows in drift wave turbulence by rotating fluid experiment (poster). 11. International congress on plasma physics, Sydney (AU), 15-19 Jul 2002. Unpublished.

Juul Rasmussen, J.; Naulin, V.; Nycander, J., Dynamics of transport barriers and ELM like behavior (talk). 2002 US Transport Task Force meeting in conjunction with the IEA Large Tokamak meeting on electron thermal transport, Annapolis, MD (US), 3-6 Apr 2002. Unpublished.

Juul Rasmussen, J.; Basu, R.; Naulin, V., Particle diffusion and density flux in anisotropic turbulence (invited talk). In: Abstracts book. International workshop on chaotic transport and complexity in classical and quantum dynamics, Carry le Rouet (FR), 24-28 Jun 2002. (PIIM, Marseilles, 2002) 1 p.

Michelsen, P.K., An overview of the Danish program (invited paper). Annual meeting of the Swedish Fusion Research Unit, Gothenburg (SE), 4-5 Nov 2002. Unpublished.

Naulin, V., Electromagnetic transport components and sheared flows in plasma edge turbulence. Spring meeting of the German Physical Society, Bochum (DE), 18-21 Mar 2002. Unpublished.

Naulin, V., Electromagnetic transport components and sheared flows (invited talk). 11. International congress on plasma physics, Sydney (AU), 15-19 Jul 2002. Unpublished.

Naulin, V., Electromagnetic transport components and sheared flows in plasma edge turbulence. Frühjahrstagung der Fachverbände Kurzzeitphysik, Plasmaphysik der Deutschen Physikalischen Gesellschaft, Bochum (DE), 18-21 Mar 2002. Verhandl. DPG (Reihe VI) (2002) v. 37 (no.5) p. 30

Naulin, V., Numerical methods for turbulence in plasmas. Lecture at Düsseldorf University, Düsseldorf (DE), 1-12 Jul 2002. Unpublished.

Naulin, V., Physics of turbulent plasma. Lecture at Charistian Albrechts University (10 x 2 hours), Kiel (DE), 4-15 Mar 2002. Unpublished.

Naulin, V., Turbulenz, Struktur und Transport (talk). MPG-IPP symposium on computational studies of turbulence in magnetised plasmas, Garching (DE), Nov 2002. Unpublished.

Naulin, V.; Basu, R.; Juul Rasmussen, J., Particle diffusion and density flux in anisotropic turbulence. In: Abstracts. International workshop: Solitons, collapses and turbulence: Achievements, developments and perspectives, Chernogolovka (RU), 18-22 Aug 2002. (L.D. Landau Institute for Theoretical Physics, Chernogolovka, 2002) 1 p.

Naulin, V.; Juul Rasmussen, J.; Nycander, J., Dynamics of transport barriers and ELM like behavior in electrostatic turbulence (poster). 11. International congress on plasma physics, Sydney (AU), 15-19 Jul 2002. Unpublished.

Naulin, V.; Juul Rasmussen, J., Electromagnetic transport components and shear flows (talk). 2002 US Transport Task Force meeting in conjunction with the IEA Large Tokamak meeting on electron thermal transport, Annapolis, MD (US), 3-6 Apr 2002. Unpublished.

Naulin, V.; Nielsen, A.H.; Juul Rasmussen, J., Turbulent equiPartion and ELM like behavior (talk). MPG-IPP theory meeting, Tegernsee (DE), Nov 2002. Unpublished.

Nielsen, A.H.; Juul Rasmussen, J.; Naulin, V.; Nycander, J., Transport barriers and ELMs in flute mode turbulence. IEA workshop on ELMs, Abingdon (GB), 24-26 Jun 2002. Unpublished.

Nielsen, A.H.; Früh, W.-G., On the origin of time-dependent behaviour in a barotropically unstable shear layer (poster). EGS 2002, 27. General assembly, Nice (FR), 21-26 Apr 2002. Geophys. Res. Abstr. (CD-ROM) (2002) v. 4

Nielsen, S.A., Elastic wave modeling by a Chebyshev collocation method. In: Book of abstracts. 28. Annual review of progress in quantitative nondestructive evaluation, Brunswick, ME (US), 29 Jul - 3 Aug 2001. (Center for Nondestructive Evaluation, Ames, IA, 2001) p. 96

Ruban, V.P.; Senchenko, S., Contour dynamics in effectively 2D ideal electron-magnetohydrodynamics flows. In: Abstracts. Workshop on turbulence and anomalous transport in plasmas and fluids, Risø (DK), 6-8 May 2002. (Risø National Laboratory, Roskilde, 2002) 1 p.

Senchenko, S.; Ruban, V.P., Contour dynamics in effective 2D ideal electro-magnehydrodynamic flows (poster). 29. European Physical Society conference on plasma physics and controlled fusion, Montreux (CH), 17-20 Jun 2002. Unpublished.

Thomsen, H.; Endler, M.; Naulin, V., Active probing experiments in Wendelstein 7-AS (poster). 11. International congress on plasma physics, Sydney (AU), 15-19 Jul 2002. Unpublished.

Verhoeven, A.G.A.; Bongers, W.A.; Elzendoorn, B.S.Q.; Graswinckel, M.; Hellingman, P.; Kamp, J.J.; Kooijman, W.; Kruijt, O.G.; Maagdenberg, J.; Ronden, D.; Stakenborg, J.; Sterk, A.B.; Tichler, J.; Alberti, S.; Goodman, T.; Henderson, M.; Hoekzema, J.A.; Oosterbeek, J.W.; Fernandez, A.; Likin, K.; Bruschi, A.; Cirant, S.; Novak, S.; Piosczyk, B.; Tumm, M.; Bindslev, H.; Kaye, A.; Fleming, C.; Zohm, H., The 113 GHz ECRH system for JET. 12. Joint workshop on electron cyclotron emission and electron cyclotron resonance heating, Aix-en-Provence (FR), 13-16 May 2002. Unpublished.

Verhoeven, A.G.A.; Bongers, W.A.; Elzendoorn, B.S.Q.; Graswinckel, M.; Hellingman, P.; Kooijman, W.; Kruijt, O.G.; Maagdenberg, J.; Ronden, D.; Stakenborg, J.; Sterk, A.B.; Tichler, J.; Alberti, S.; Goodman, T.; Henderson, M.; Hoekzema, J.A.; Oosterbeek, J.W.; Fernandez, A.; Likin, K.; Bruschi, A.; Cirant, S.; Novak, S.; Piosczyk, B.; Tumm, M.; Bindslev, H.; Kaye, A.; Fleming, C.; Zohm, H., The design and R and D of an ECRH system on JET (poster). 22. Symposium on fusion technology, Helsinki (FI), 9-13 Sep 2002. Unpublished.

Westerhof, E.; Hogeweij, G.M.D.; Hoekzema, J.A.; Schüller, F.C.; Barth, C.J.; Bindslev, H.; Donné, A.J.H.; Dumortier, P.; Gorkom, J.C. van; Jaspers, R.J.E.; Kalupin, D.; Koslowski, H.R.; Krämer-Flecken, A.; Cardozo, N.J.L.; Meiden, H.J. van der; Messiaen, A.; Oyevaar, T.; Polman, R.W.; Porte, L.; Udientsev, V.S.; Unterberg, B.; Vervier, M.; Eester, D. van; Wassenhove, G. van, Electron cyclotron resonance heating on TEXTOR: Results from the preliminary 110 GHz system. 12. Joint workshop on electron cyclotron emission and electron cyclotron resonance heating, Aix-en-Provence (FR), 13-16 May 2002. Unpublished.

Westerhof, E.; Hogeweij, G.M.D.; Hoekzema, J.A.; Schüller, F.C.; Barth, C.J.; Bindslev, H.; Donné, A.J.H.; Dumortier, P.; Gorkom, J.C. van; Jaspers, R.J.E.; Kalupin, D.; Koslowski, H.R.; Krämer-Flecken, A.; Cardozo, N.J.L.; Meiden, H.J. van der; Messiaen, A.; Oyevaar, T.; Polman, R.W.; Porte, L.; Udientsev, V.S.; Unterberg, B.; Vervier, M.; Eester, D. van; Wassenhove, G. van, Electron cyclotron resonance heating with the preliminary 110GHz system on TEXTOR. 5. International workshop on strong microwaves in plasmas, Nizhny Novgorod (RU), 1-9 Aug 2002. Unpublished.

2.15.7 Internal reports and patent applications

Bindslev, H., Assessment of the JT60-U CO_2 CTS, Internal report to IEA. (2002) vp.

3. Fusion technology

3.1 Introduction

The work reported in this section has been carried out in the Materials Research Department. The overall objective of the research activities in this area is to determine the impact of neutron irradiation on physical and mechanical properties of metals and alloys, so that appropriate materials can be chosen for their application in an irradia-tion environment (e.g. in a fusion reactor). Various experimental techniques are employed to study different aspects of the microstructural evolution during irradiation and the resulting consequences of the post-irradiation physical and mechanical properties of metals and alloys. Calculations and computer simulations are performed to understand the evolution of surviving defects and their clusters in collision cascades. The kinetics of defect accumulation during irradiation and the influence of irradiation-induced defects and their clusters on the deformation behaviour of irradiated metals and alloys are studied theoretically. In the following, the main results of these activities are highlighted.

3.2 Next step technology

3.2.1 Creep-fatigue cyclic deformation and lifetime of copper alloys[1]

B.N. Singh, M. Li and J.F. Stubbins* (*University of Illinois, Urbana-Chamaign, USA)*

Both the dispersion strengthened Glid Cop CuAl-25 and the precipitation hardened CuCrZr alloys are still being evaluated for their potential application in the first wall and divertor components of ITER. In the reactor vessel these materials will be exposed to fusion neutrons and will experience thermo-mechanical cyclic loading as a result of the cyclic nature of plasma burn operations of the system. Because of the "plasma-on" and "plasma-off" mode of operation, these materials will also experience the stress relaxation and microstructural recovery (i.e. creep). In other words, the deformation behaviour and performance of these materials will be affected by processes operating during the cyclic loading (i.e. fatigue) and during the stress relaxation period (i.e. creep). Very little is known about the impact of this creep-fatigue interaction on the mechanical response of metals and alloys. In order to evaluate the impact of this interaction, investigations were initiated two years ago. These investigations have been continued and the main results are briefly summarized in the following. It should be pointed out that the present work has concentrated more on CuCrZr alloy since this alloy is considered to be more suitable for ITER application and offers the possibility of improving its performance by appropriate thermo-mechanical heat treatments.

Materials used in the present investigations were a dispersion strengthened copper alloy, Glid Cop CuAl-25 (LOCL) and two types of precipitation hardened CuCrZr alloys, one supplied by Tréfimétaux (France) and the other by Outokumpu (Finland). The Tréfimétaux CuCrZr alloys was used only in the prime aged condition (CuCrZr E alloy) whereas Outokumpu CrCrZr alloy was used in the prime aged (CuCrZr PA) as well as overaged

[1] Task GB8-V63 (BL 12.2) and TWO-T507-5

(CuCrZrHT1) conditions. The overageing was achieved by the heat treatment of CuCrZr PA at 600^{o}C for one hour.

A number of fatigue specimens of these materials were fatigue tested in a strain controlled mode in a servo-electrical mechanical test stand. The loading cycles were always fully reversed (i.e. R = -1) so that the maximum tension strain was the same as the maximum compressive strain. The loading frequency was 0.5 Hz. The creep-fatigue interaction condition was simulated by applying a certain holdtime on either tension, compression or both tension and compression sides of the cyclic loading. Holdtimes of 2 and 5 seconds were used. The specimens tested with and without holdtimes were cycled to failure. For a given holdtime, the number of cycles to failure was determined at different strain amplitudes. All tests were carried out at room temperature.

Figure 1a shows results of room temperature tests on Glid Cop CuAl-25 without holdtime (i.e. fatigue) as well as with holdtime (i.e. creep-fatigue) of 2 and 10 seconds. It can be seen that the number of cycles to failure (i.e. the lifetime) of specimens decreases with increasing strain amplitude. It can be also seen that the number of cycles to failure is lower in the case of creep-fatigue tests than that in the case of monotonic fatigue tests. It is of interest to note that this reduction in the number of cycles to failure increases with decreasing strain amplitude. This is further illustrated in Fig. 1b showing that the ratio of the number of cycles to failure with holdtime (N^{hold}) to the number of cycles to failure without holdtime ($N^{no\ hold}$) decreases with decreasing strain amplitude. At present there seems to be no clear explanation for this effect.

The strain amplitude dependence of number of cycles to failure determined at room temperature for the prime aged CuCrZr alloy is shown in Fig. 2a. The results for tests with and without holdtime are shown. Figure 2a also includes the results of additional tests where the holdtime was applied only in the tension (TH) and only in the compression (CH) side of the cyclic loading. Note that TCH refers to those tests where the holdtime was applied on both the tension and the compression sides of the cyclic loading.

First of all it should be noted that the number of cycles to failure at a given strain amplitude is lower for the CuCrZr (PA) alloy than that for the Glid Cop CuAl-25 alloy. Furthermore, this reduction becomes even larger at decreasing strain amplitude (see Fig. 2a). The decrease in the ratio ($N^{hold}/N^{no\ hold}$) with strain amplitude is weaker in the case of CuCrZr (PA) than in the case of Glid Cop CuAl-25 (see Fig. 2b). In other words, the CuCrZr (PA) appears to be less sensitive to holdtime (i.e. creep-fatigue interaction). In view of the scatter in the results obtained, it remains unclear as to whether or not the only tension (TH) and only compression (CH) modes of maintaining holdtimes yield longer lifetime than that in the case of tension-compression (TCH) holdtime.

Some limited number of tests have been carried out to investigate the effect of heat treatment and composition of CuCrZr alloys. Figure 3 shows the results for the overaged (600^{o}C/1 h) Outokumpu CuCrZr (HT1) alloy and the prime aged Tréfimétaux CuCrZr (E) alloy. Clearly, the CuCrZr (HT1) alloy yields higher number of cycles to failure at the higher strain amplitudes than that in the case of CuCrZr (E) alloy. This behaviour reverses, on the other hand, at lower strain amplitudes. These results also indicate that although CuCrZr (E) alloy may be sensitive to the holdtime (i.e. creep-fatigue) effect, the CuCrZr (HT1) alloy may not suffer from the adverse effects of creep-fatigue interaction. These results may be taken to suggest that the effects of creep-fatigue interaction may be circumvented by modifying the initial microstructure by heat treatments or thermo-mechanical treatments.

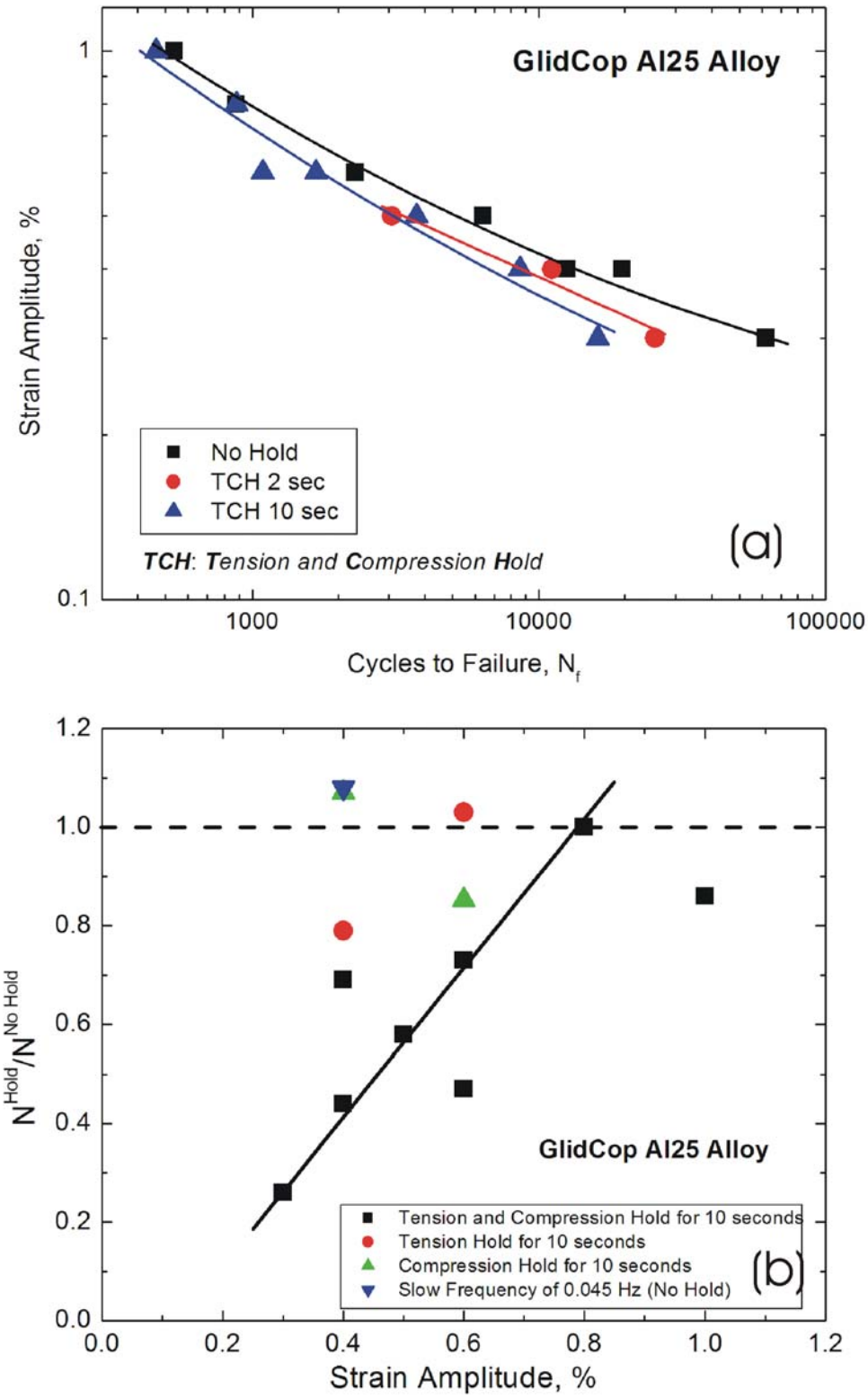

Figure 1. (a) Number of cycles to failure (N_f) as a function of strain amplitude (% per cycle) for Glid Cop Al-25 (LOCL) alloy fatigue tested at room temerature with no holdtime and tension and compression holdtimes of 2 and 10 seconds; (b) ratio of cycles to failure with holdtime (N^{hold}) and without holdtime ($N^{no\ hold}$) as a function of strain amplitude.

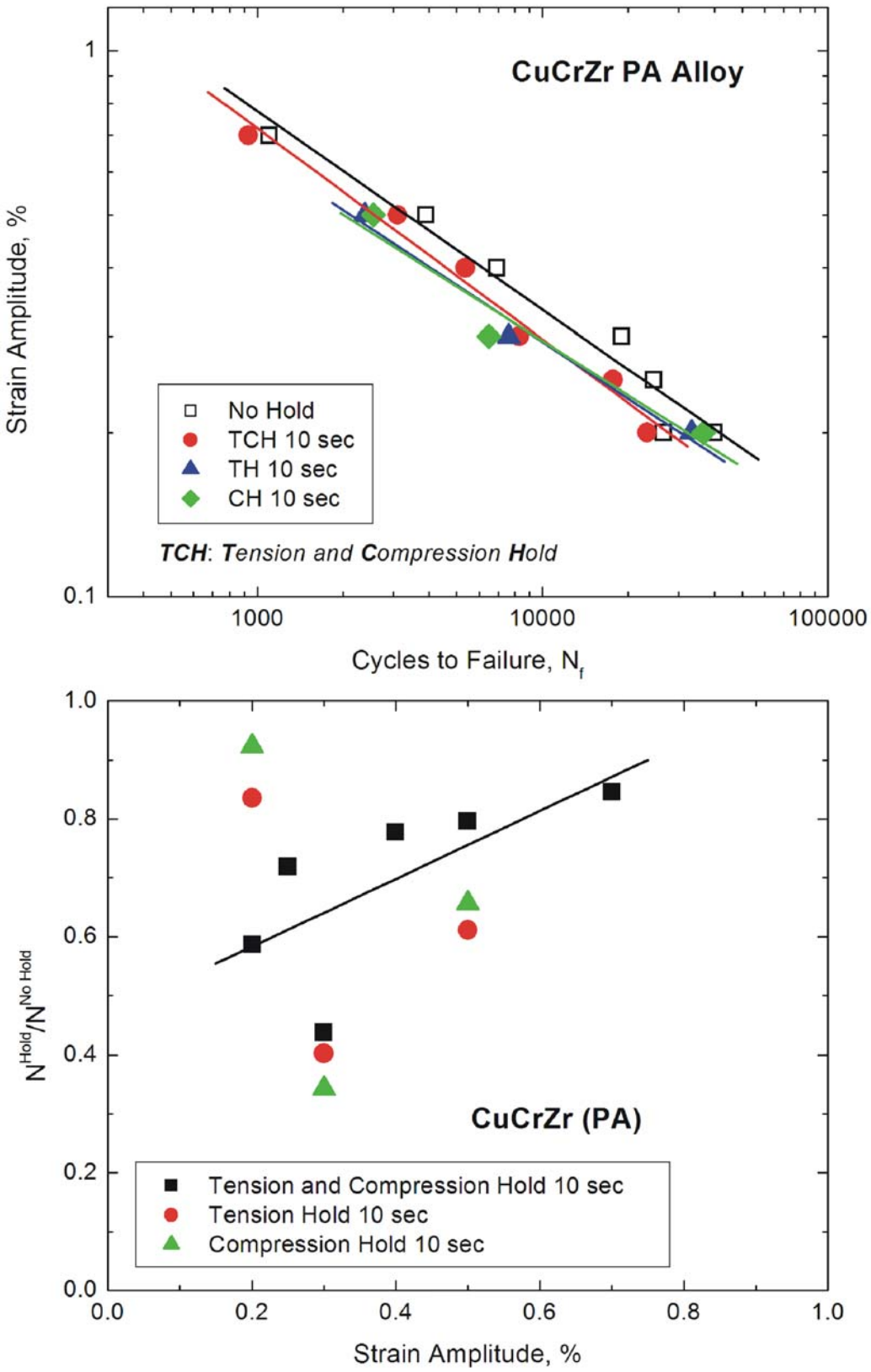

Figure 2. Same as Figure 1 but for CuCrZr alloy; TH, CH and TCH refer, respectively, to holdtime only in tension, holdtime only in compression and holdtime both in tension and compression sides of the cyclic loading.

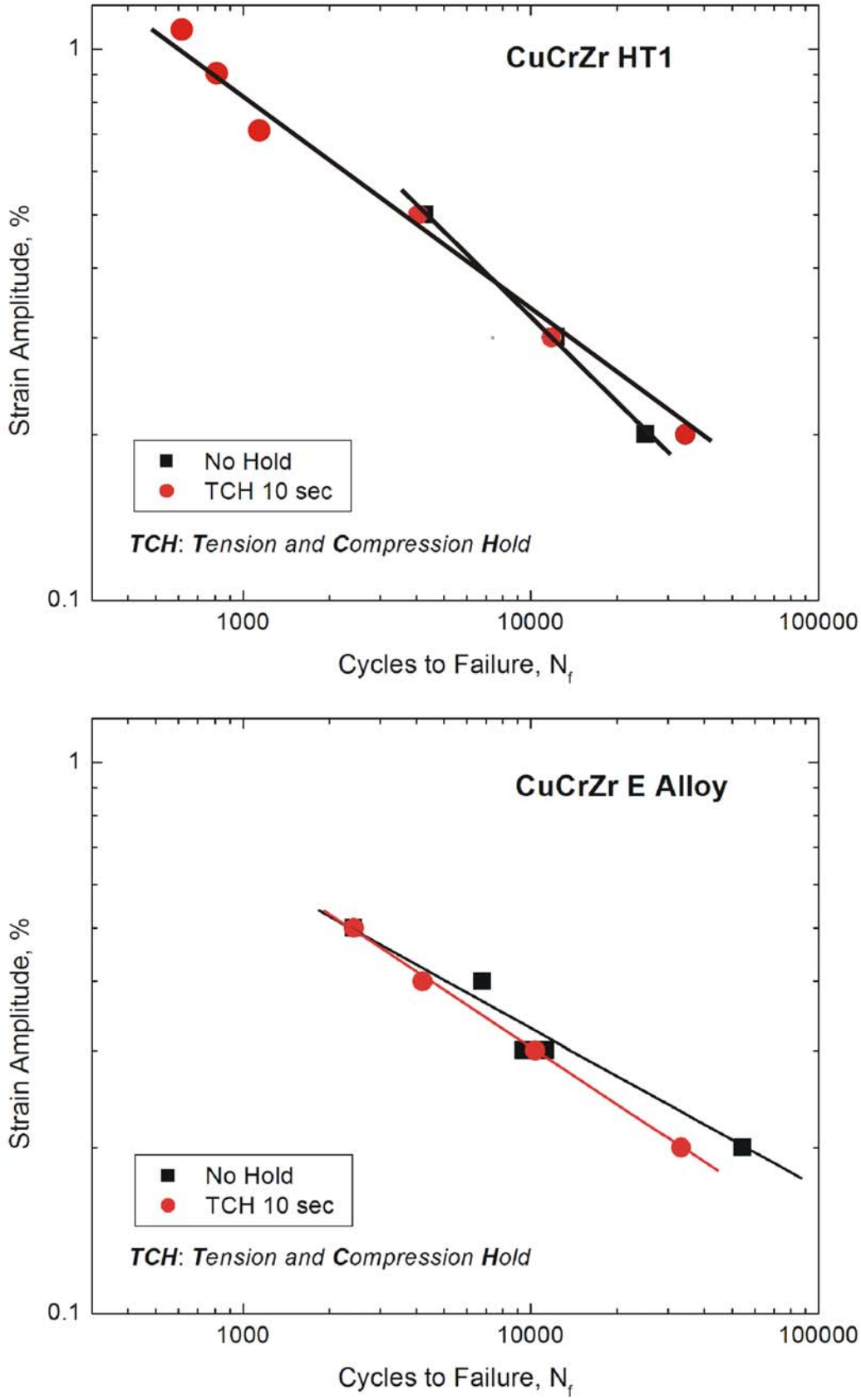

Figure 3. Number of cycles to failure (N_f) as a function of strain amplitude (% per cycle) for (a) overaged Outokumpu (CuCrZr HT1) alloy and (b) prime aged Tréfimétaux CuCrZr (E) alloy tested with a tension and compression holdtime (TCH) of 10 seconds at room temperature.

3.2.2 Influence of pre-irradiation heat treatment on mechanical properties of CuCrZr alloy[2]

B.N. Singh, D.J. Edwards[*] ([*]Pacific Northwest National Laboratory, Richland, USA) and P. Toft

The precipitation hardened CuCrZr alloy is being seriously evaluated for its possible use in the first wall and divertor components of ITER. Neutron irradiation of this alloy in the prime aged condition at temperature below 200°C has been found to make this alloy plastically unstable. Post-irradiation deformation is found to be dominated by plastic flow localization, lack of work hardening and uniform elongation. These features have been matters of concern from the point of view of practical application of this alloy in ITER. It was, therefore, decided to alter the pre-irradiation precipitate microstructure by heat treatments. The results on microstructural modifications due to various heat treatments and their effect on tensile properties at 50 and 300°C in the unirradiated condition were reported last year. In the following the main results on the effect of neutron irradiation on the microstructure and deformation behaviour of the CuCrZr alloy with different pre-irradiation heat treatments are briefly described.

A number of tensile specimens of CuCrZr alloy in the prime aged condition and specimens heat treated after prime ageing at 600°C for 1 and 4 hours were irradiated with fission neutrons in the BR-2 reactor at Mol (Belgium) at 60 and 300°C to a displacement dose level of 0.3 dpa. The specimens irradiated at 60°C were tensile tested at 22 and 60°C whereas those irradiated at 300° were tensile tested at 300°C. The results are illustrated in Figs. 4 and 5 for the test temperatures of 60 and 300°C, resectively.

As reported last year, both overageing heat treatments of the prime aged CuCrZr alloy led to reductions in the yield strength of the alloy. Irradiation at 60°C to a dose level of ~0.3 dpa causes a moderate amount of increase in the yield strength of the prime aged as well as overaged alloys. The increase in the yield strength is, however, accompanied by a substantial decrease in the ductility of the irradiated CuCrZr alloy with different pre-irradiation heat treatments. What is most significant and important from the application point of view, however, is the observation that the irradiation at 60°C to 0.3 dpa does not cause any noticeable yield drop and plastic instability following the lower yield stress. For a direct comparison, the results of earlier irradiation and deformation experiments at 100°C showing drastic yield drop and plastic instability are shown in Fig. 6. It should be pointed out, however, that although the overageing heat treatments have eliminated the technological problem of plastic instability at the very beginning of the plastic defomation (see Fig. 6), the irradiated alloy still suffers from the lack of work hardening and a decrease in ductility. Some further adjustment of the pre-irradiation microstructure may be attempted to address these problems.

The results of irradiation and the post-irradiation tensile testings at 300°C shown in Fig. 5 demonstrate that the CuCrZr alloy both in the prime aged and overaged conditions becomes noticeably softer due to irradiation at 300°C.

[2] Task TWO-T507-6

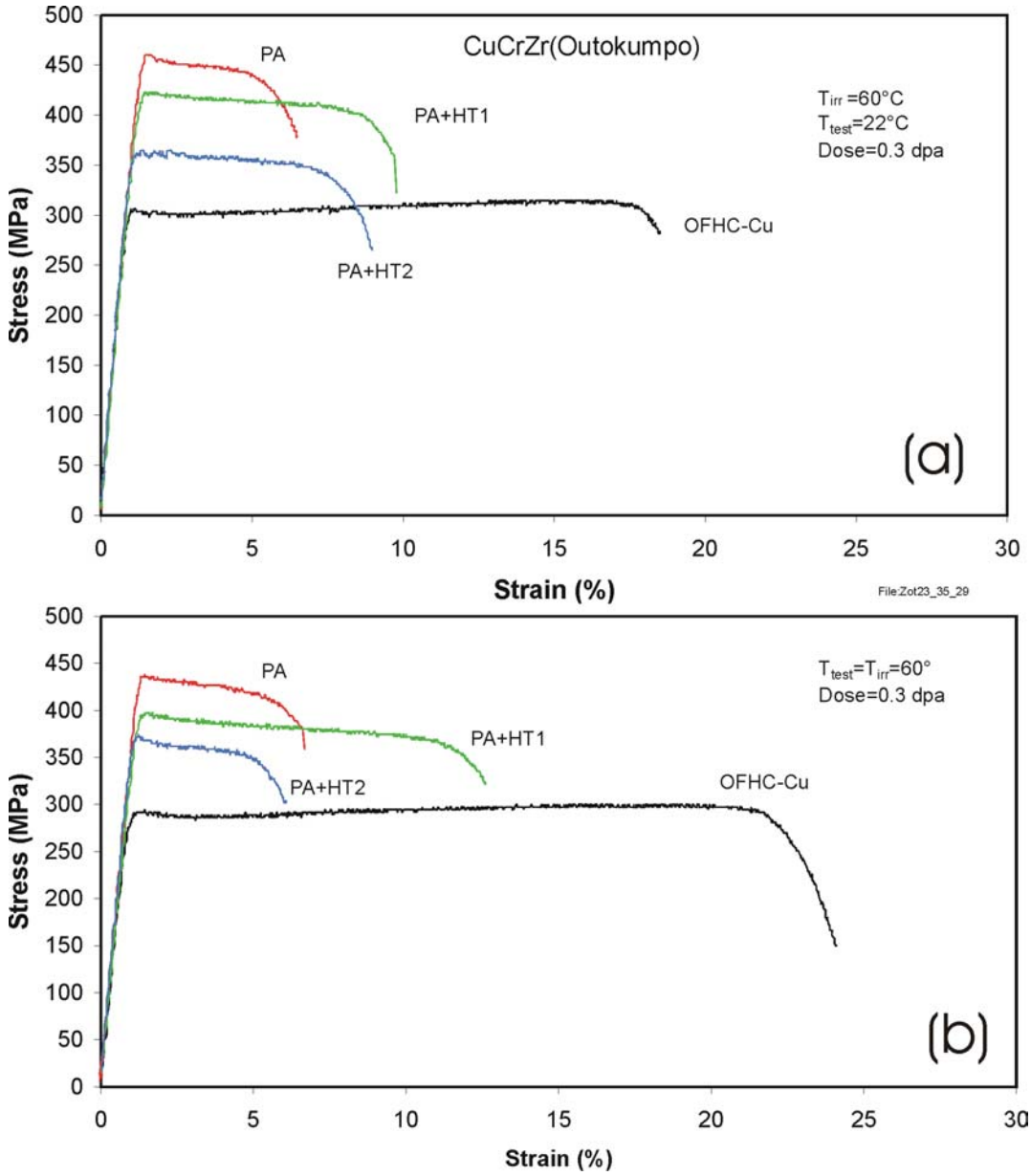

Figure 4. Stress-strain curves for Outokumpu CuCrZr alloy irradiated at 60°C to a dose level of 0.3 dpa in the prime aged and overaged (at 600°C for 1 h (PA + HT1) and 4 h (PA + HT2)) conditions and tensile tested at (a) 22°C and (b) 60°C.

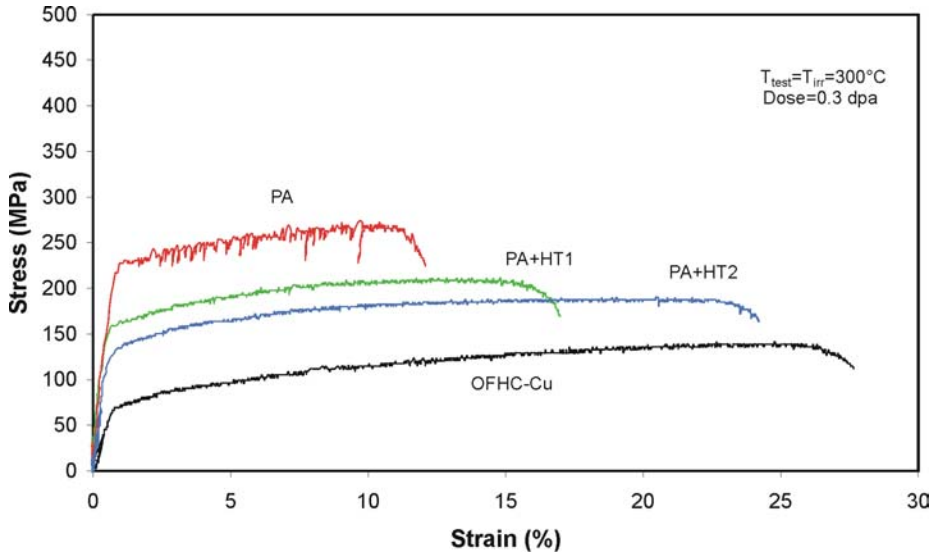

Figure 5. Same as Figure 4 but irradiated and tensile tested at 300°C.

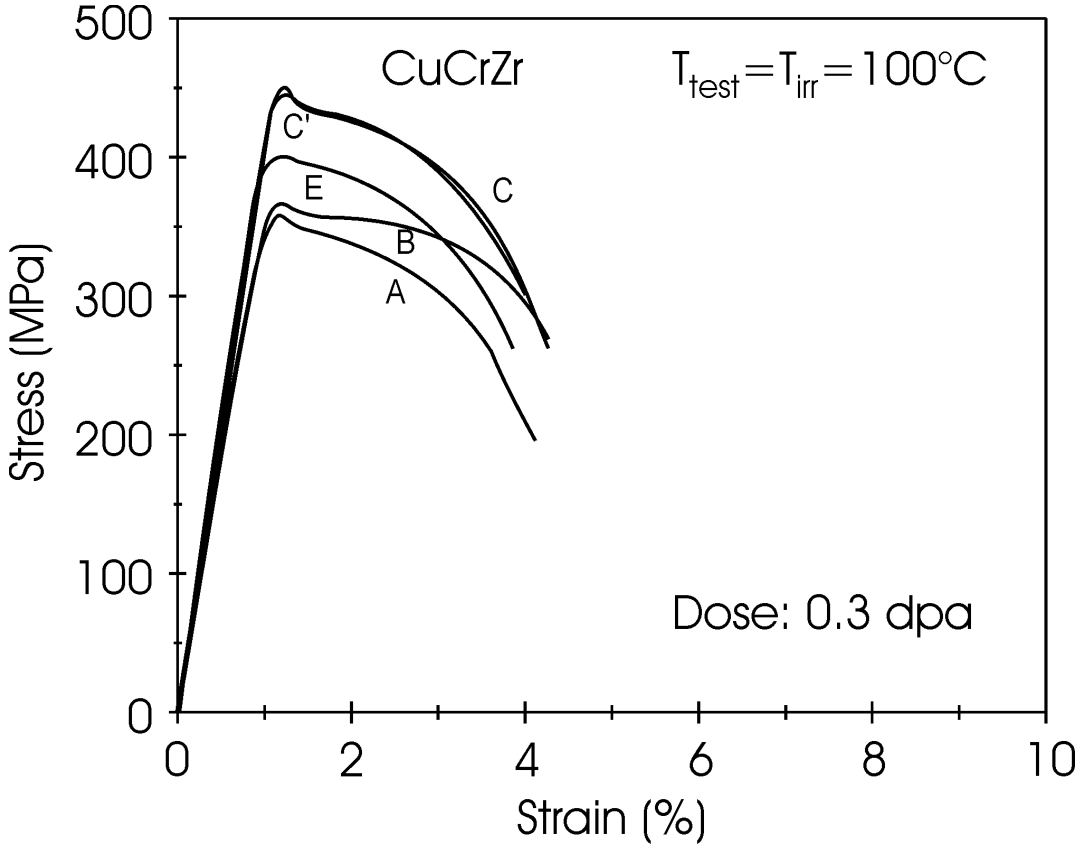

Figure 6. Stress-strain curves for Tréfimétaux CuCrZr alloy (with different heat treatments) irradiated (0.3 dpa) and tensile tested at 100°C.

Microstructures of the CuCrZr alloy with different heat treatments irradiated at 60 and 300°C to 0.3 dpa have been investigated using transmission electron microscoy in the as-irradiated as well as in the irradiated and deformed conditions. Even though none of the irradiated specimens exhibited any noticeable yield drop and plastic instability, the evidence of plastic flow localization in the form of cleared channels was found in all of the irradiated and deformed specimens. The localized deformation in the cleared channels may be responsible for the lack of work hardening as well as the reduction in the ductility of specimens irradiated at 60°C.

3.2.3 In-reactor tensile testing of pure copper at 90°C in the BR-2 reactor at Mol[3]

B.N. Singh, S. Tähtinen, P. Moilanen* (*VTT Industrial Systems, Espoo, Finland),*
*P. Jacquet** and J. Dekeyser** (**Reactor Experiments-TCH, SCK·CEN, Mol, Belgium)*

It has been a common practice for more than 40 years to assess the effect of neutron irradiation on mechanical properties of metals and alloys on the basis of results obtained from post-irradiation deformation experiments. The materials employed in the structural components of a fission or fusion reactor, on the other hand, will be exposed simultaneously to external stresses and irradiation induced defect population produced continuously during irradiation. Under these conditions, both the magnitude and the spatial distribution of defect accumulation and hence the deformation behaviour may be substantially different from that in the case of post-irradiation experiments (see later for further details). This raises a serious question as to whether or not the results and the conclusions of the post-irradiation deformation experiments can be taken to represent the behaviour of materials used in the structural components of a nuclear or thermonuclear reactor. In our view, this question can be answered properly and reliably only by determining experimentally the deformation behaviour of materials subjected simultaneously to plastic deformation and neutron irradiation. In order to address this problem, recently we have carried out in-reactor deformation experiments and have determined the dynamic stress-strain curves for pure copper subjected simultaneously to plastic deformation and neutron irradiation at ~90°C.

The material used in the present investigation was thin (0.3 mm) sheet of oxygen-free high conductivity (OFHC) copper containing 10, 3, <1 ppm, and <1 ppm, respectively, of Ag, Si, Fe and Mg. The oxygen content of this copper was found to be 34 appm. Tensile samples of polycrystalline OFHC-copper were annealed at 550°C for 2h in a vacuum of 10^{-9} bar. The resulting grain size and dislocation density were about 30 μm and $\leq 10^{12}$ m^{-2}, respectively. These annealed specimens were used in the uniaxial tensile testing experiments performed inside the BR-2 reactor at Mol.

The tensile test was carried out in a specially designed pneumatically controlled test module. The module was constructed and calibrated (out-of-pile) at VTT. The applied stress and the resulting strain on the specimen was measured continuously throughout the whole experiment both in the case of out-of-pile and in-reactor tests. The temperature of the experiment was also monitored and recorded continuously. The in-reactor tensile test was carried out at ~90°C with a fast neutron flux of ~3 x 10^{17} n/m^2s (E>1 MeV) corresponding to a displacement damage rate of 6 x 10^{-8} dpa/s. The specimen was deformed at a strain rate of 1.3 x 10^{-7} s^{-1} (~1.1% per day). This low strain rate was chosen to ensure that the specimen should survive the in-reactor deformation for long enough time to accumulate a displacement dose level of about 0.1 dpa. This was necessary in order to assess the dynamic effects of irradiation and the applied stress on the deformation behaviour of the specimen. The tensile

[3] Task TW2-TVV-SITU

test was discontinued soon after the specimen showed a clear sign of necking (i.e. before fracture). The test rig was then taken out of the reactor.

Figure 7 shows the dynamic response of the material to the applied stress (necessary to maintain the strain rate of $1.3x10^{-7}s^{-1}$) and the neutron irradiation. Clearly, in the beginning there is a rapid increase in the stress level with increasing strain and the displacement dose level which then slows down and finally saturates. Soon after the saturation, the stress begins to decrease indicating the onset of necking and failure. As can be seen in Fig. 7, under the present testing conditions the specimen reaches uniform elongation value of ~12.5%. It should be pointed out that the hardening (i.e. increase in the stress level) observed in the present experiments is due to strain hardening as well as the hardening induced by the lattice defects and their clusters generated continuously during irradiation. The most significant feature of the present experiment is that during the dynamic in-reactor test, the material deforms uniformly and in a homogeneous fashion and does not show any sign of yield drop and plastic instability (i.e. low temperature embrittlement) as commonly demonstrated by the post-irradiation experiments.

Figure 7 also shows the displacement damage (Fig. 7a) and the time dependence of the applied strain (Fig. 7c) accumulated in the tensile specimen.

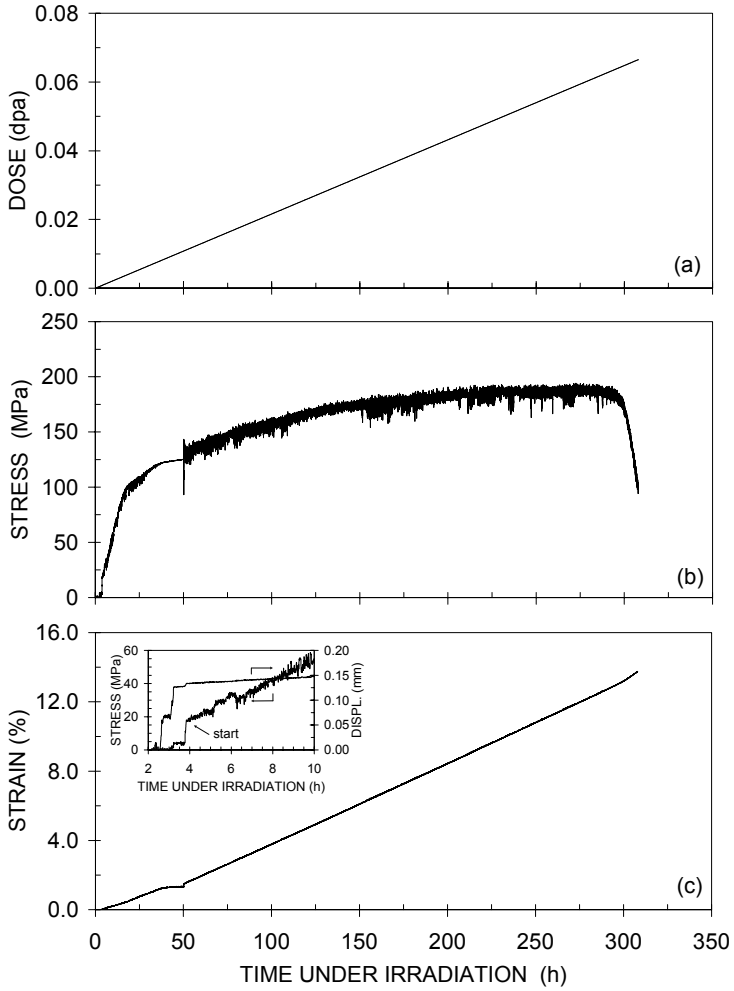

Figure 7. In-reactor uniaxial tensile test results showing a) irradiation dose, b) stress and c) strain as a function of time under neutron irradiation.

3.3 Long-term technology

3.3.1 Effect of neutron irradiation on defect accumulation and tensile properties of iron, F82H and Eurofer-97 steels[4]

B.N. Singh, M. Eldrup and P. Toft

Effect of neutron irradiation on physical and mechanical properties of low activation ferritic-martensitic steels are being extensively studied internationally since these alloys are considered to be candidate materials for the blanket and first wall of fusion reactors (e.g. DEMO). Although these alloys are resistant to void swelling and maintain good fracture toughness at irradiation temperatures above about 400°C, they are prone to loss of ductility at lower irradiation temperatures. Furthermore, it has also been shown recently that even at these low temperatures void formation may readily occur in bcc crystals. Very little is known, on the other hand, about the mechanisms controlling the loss of ductility or void formation at low temperatures in these steels. The recent work is a part of the European activities devoted to mechanistic studies of damage accumulation, irradiation hardening and loss of ductility.

Tensile specimens of pure iron (annealed at 650°C for 2 hours in vacuum), F82H and EUROFER-97 steels were irradiated with fission neutrons in the BR-2 reactor at Mol (Belgium) at 60 and 300°C to a dose level of ~0.23 dpa. The irradiated specimens were tensile tested at 60 and 300°C with a strain rate of 1.3×10^{-3} s^{-1}. Figs. 8 and 9 show the stress-strain curves for pure iron, F82H and EUROFER-97 steels tested at 60 and 300°C, respectively, both in the unirradiated and irradiated conditions. The results lead to the following preliminary conclusions: (a) that the irradiation at 60°C even to this low displacement damage level of only about 0.23 dpa, causes a significant decrease in the uniform elongation of both F82H and Eurofer-97 steels, (b) that the irradiation at 300°C to ~0.23 dpa has practically no effect on the mechanical performance of these steels and (c) that the uniform elongation of both F82H and EUROFER-97 is lower at 300°C than that at 60°C both in the unirradiated and irradiated conditions.

3.3.2 A comparison of helium implanted iron and Eurofer97: effects of He dose[5]

M. Eldrup, B. N. Singh and P. Jung (*Institut für Festkörperforschung, Forschungszentrum Jülich, Association EURATOM-FZJ, Germany)*

This work is part of an effort to investigate, experimentally as well as theoretically, the role of He in cavity nucleation in neutron irradiated iron and steel. We have previously reported results on cavity formation at low temperatures and at low neutron doses in iron and steel without He-implantation.

Strip specimens ($20 \times 3 \times 0.1$ mm^3) and dog-bone shaped 20 mm long tensile specimens (with gauge length and width 8 and 3 mm, respectively) of pure iron and EUROFER97 steel were homogeneously implanted with He. The implantations took place at 50°C to doses of 1, 10 and 100 atppm and at 350°C to doses of 10 and 100 atppm at a rate of 2×10^{-2} appm He/s, equivalent to a displacement damage rate of 3.1×10^{-6} dpa/s. The microstructure after He implantation was investigated by Positron annihilation spectroscopy (PAS), which is sensitive to cavities in the size range from single vacancies to several nano-metres.

[4] Task TTMS-001
[5] Task TTMS-001

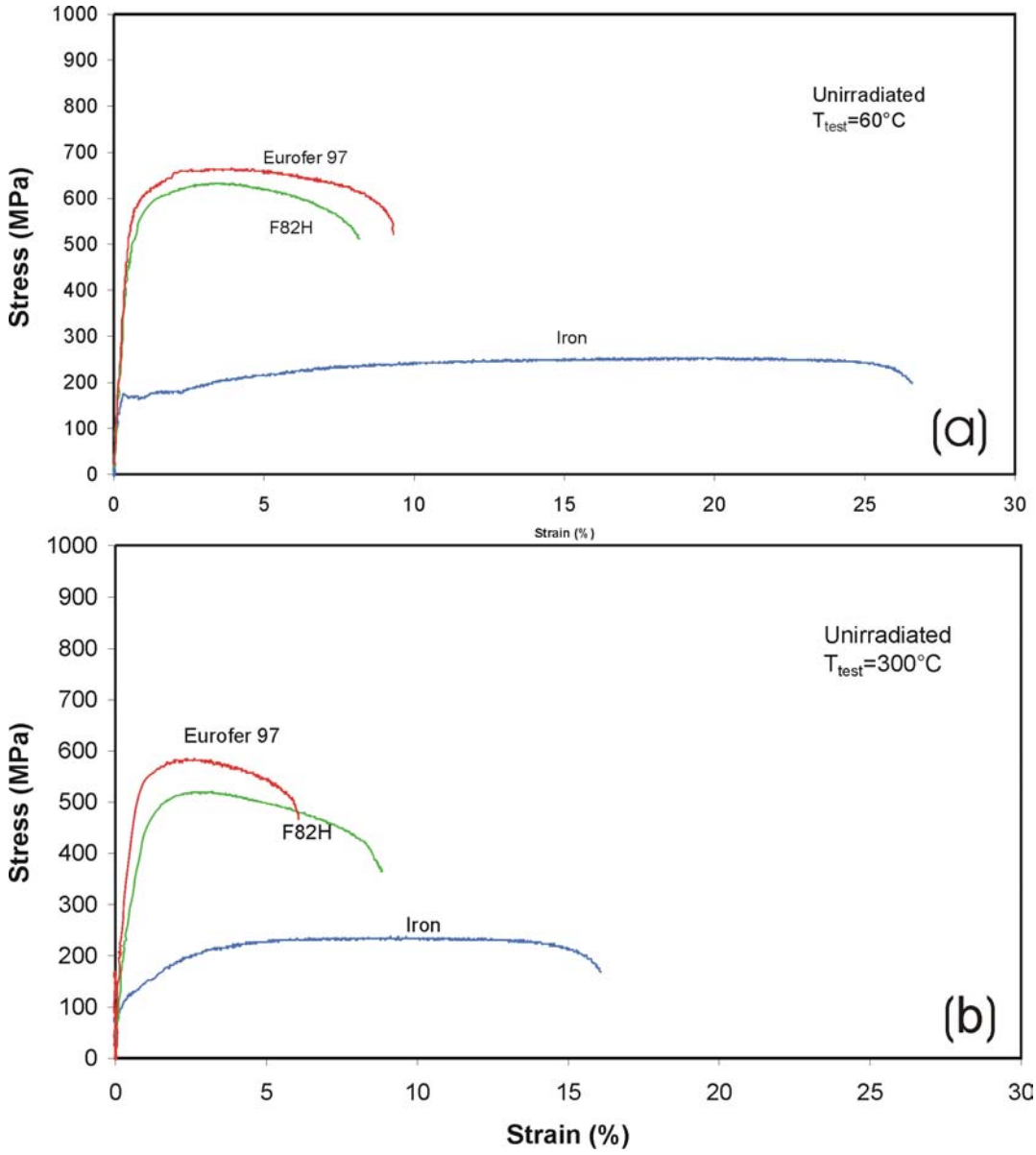

Figure 8. Stress-strain curves for pure iron, F82H and EUROFER97 steels tested at (a) 60°C and (b) 300°C.

The PAS results show that like in the case of neutron irradiation, nano-cavities are formed during He implantation both in pure Fe and in EUROFER97 at 50°C (Fig. 10) as well as at 350°C. In the case of pure Fe at 50°C, the He does not seem to enhance the cavity nucleation in any significant way compared to neutron irradiation to the same displacement damage level, even when 100 atppm He are implanted. In the case of EUROFER97, however, the cavity nucleation at 50°C appears to be less efficient than that in pure iron (Fig. 10). The difference in efficiency of cavity nucleation between iron and EUROFER97 is found to be smaller at 350°C than at 50°C: For example, the density of the observed cavities in EUROFER97 is estimated to be two to three times smaller than in Fe (100atppm He, 350°C).

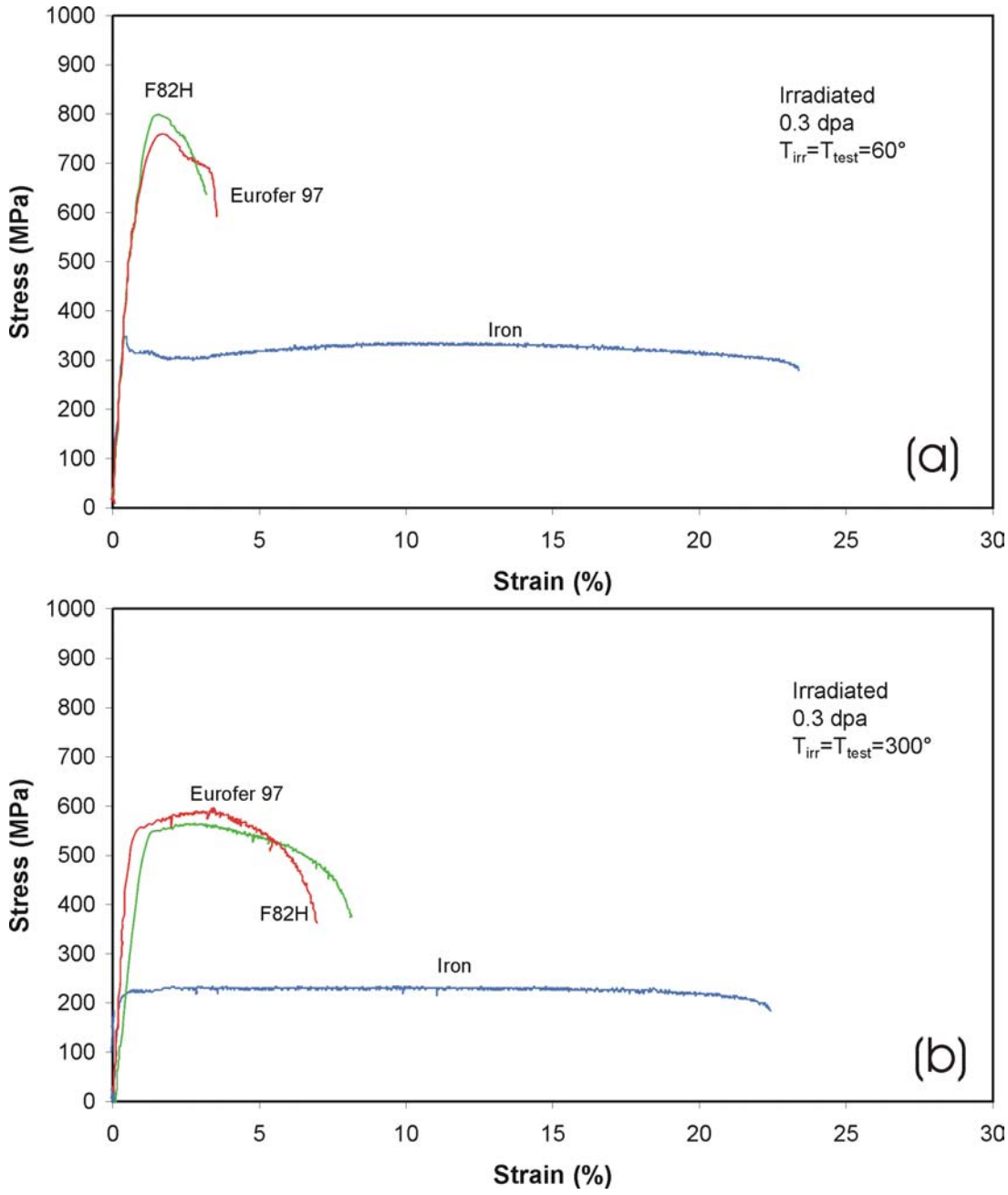

Figure 9. Same as Figure 8 but tested after irradiation at a 60°C and (b) 300°C to a dose level of 0.23 dpa.

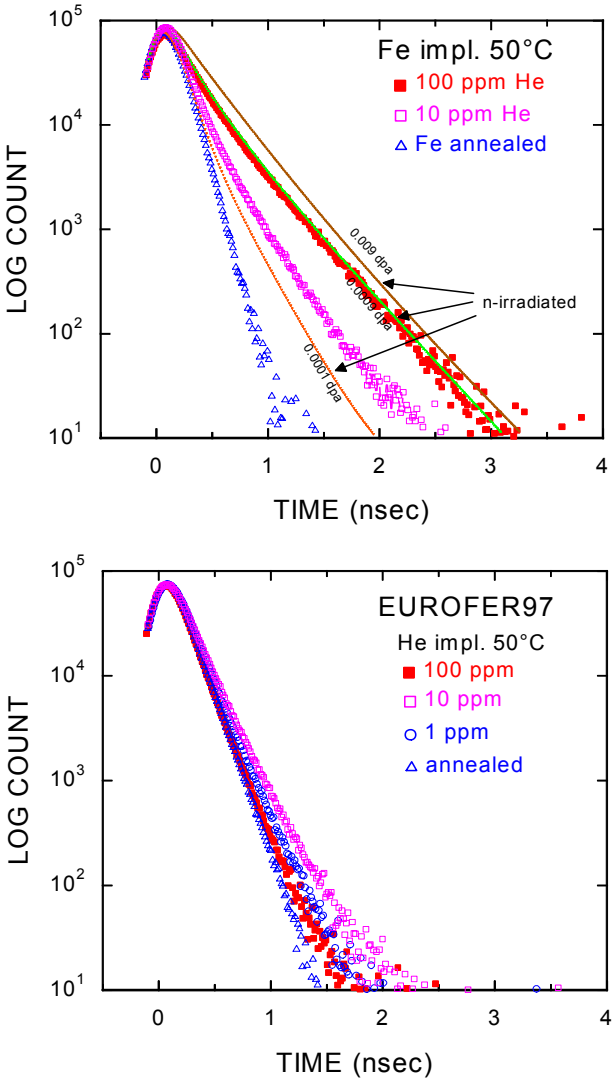

Figure 10. Comparison of positron lifetime spectra for He-implanted Fe and EUROFER97. In both materials the He implantation gives rise to an increase in positron lifetimes, due to bubble formation. Clearly, the effect of implantation is bigger in Fe than in EUROFER97. In the upper part of the figure, the spectra for He-implanted Fe are compared with spectra for neutron irradiated Fe. The spectra are similar, but for comparable displacement damage doses, spectra for He-implantation are somewhat below those for neutron irradiation (implantation with 10 and 100 ppm He leads to displacement damage doses of 0.0015 and 0.015 dpa, respectively).

The next step in the present project will be to study the influence of neutron irradiation on the as-implanted Fe and EUROFER97. This work is in progress.

The results mentioned above are semi-quantitative in nature. In order to obtain more accurate quantitative data on size and density of cavities/bubbles formed during He implantation, one important factor will be to determine the influence of He atoms in very small bubbles (smaller than roughly 1 nm) on positron lifetimes and trapping efficiencies.

3.3.3 **Dynamic properties of edge dislocation decorated by interstitial loops in iron and copper**[6]

Yu. N. Osetsky, D.J. Bacon* (University of Liverpool, Liverpool, UK) and B. N. Singh*

Thermally-activated one-dimensional glide of clusters of self-interstitial atoms (SIAs) has been observed by atomistic simulations in bcc iron as well as fcc copper. In bcc iron practically all SIA clusters produced in displacement cascades are glissile whereas in fcc copper both glissile and sessile clusters of SIAs are produced. In both cases the glissile clusters are expected to cause decoration of grown-in dislocations by loops of SIAs. According to the cascade-induced source hardening (CISH) model[7], dislocation decorations are considered to be responsible for a significant increase in the yield strength and for the phenomena of yield drop and plastic flow localization in metals and alloys irradiated under cascade damage conditions (e.g. in a fission or fusion reactor). These calculations are, however, based on isotropic elasticity theory and assumes the dislocation line to be static and rigid.

In real experiments, on the other hand, the dislocations are likely to be mobile and flexible. It is, therefore, of interest to simulate the dynamic properties of dislocations decorated with small SIA loops. In the present work, the details of interactions between moving dislocations and SIA clusters have been investigated using molecular dynamics simulations at zero and 300K. The results of the atomic-scale simulations are compared with the results of calculations based on the continuum elasticity theory. In the simulation periodic array of edge dislocations are considered. Both bcc and fcc crystals contain about 750.000 atoms. Many-body interatomic potentials of Finnis-Siclar type is used. The Burgers vector of the SIA loops is taken to be the same as that of the edge dislocation. The crystal containing the edge dislocation decorated with a set of SIA loops of sizes between 0.5 and 2.5 nm is strained at a strain increament of 10^{-4}.

The preliminary results demonstrate that the static interactions can be described by continuum elasticity theory although the dynamics of the decorated dislocations requires atomic-scale simulations such as molecular dynamics. The results also show that the edge dislocation in bcc iron moves faster and has correspondingly lower drag coefficient than that in fcc copper (Fig. 11). These differences are due to the difference in the structure of the non-dissociated dislocation in iron and the dissociated dislocation in copper. Thus, it follows that kinetic effects in iron should be more significant than that in copper.

[6] Task TTMS-001

[7] B.N. Singh, A.J.E. Foreman and H. Trinkaus, J. Nucl. Mater. 251 (1997) 103

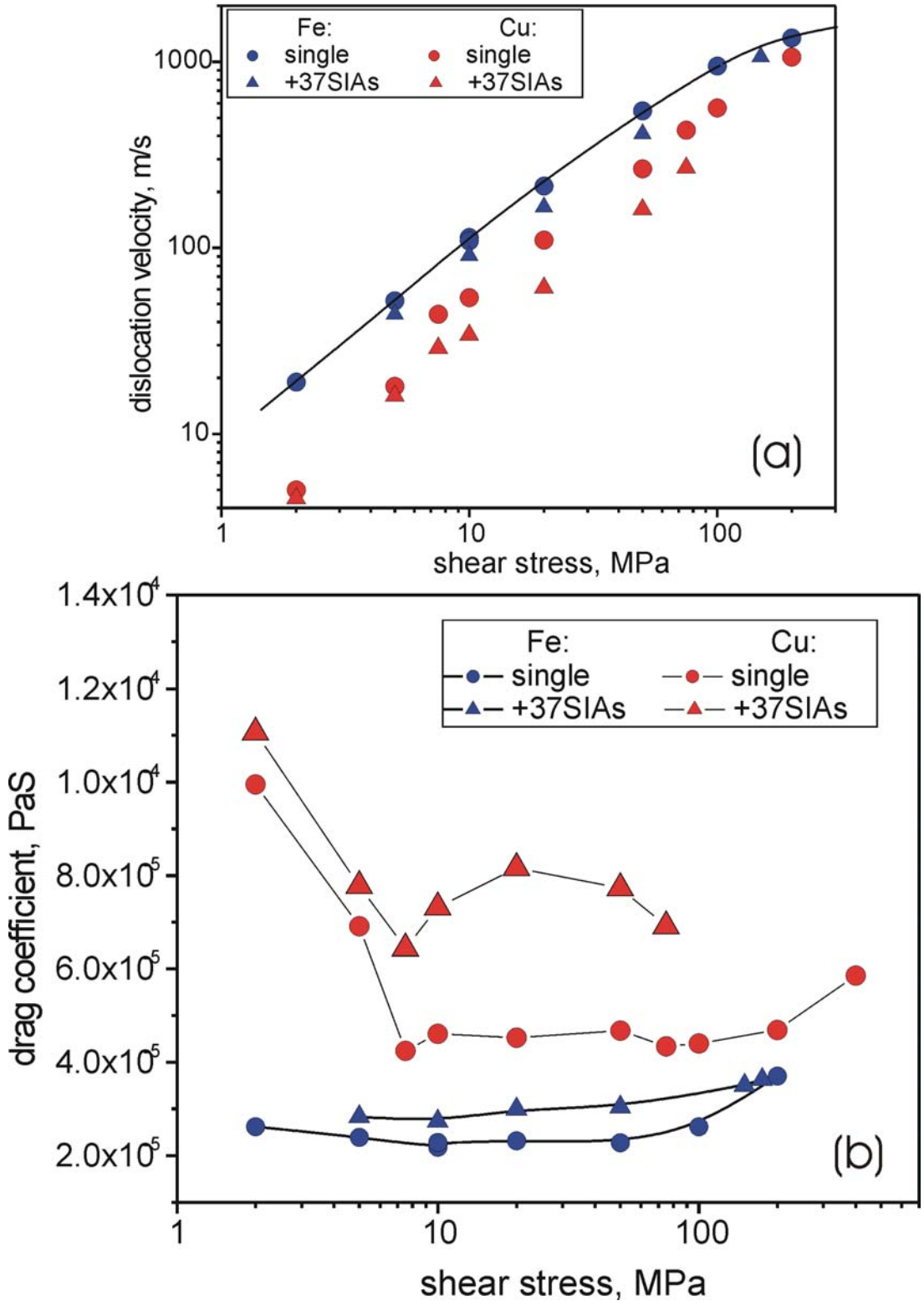

Figure 11. Results of molecular dynamic simulations showing the effect of stress on (a) dislocation velocity and (b) drag coefficient for edge dislocations decorated with interstitial clusters in iron and copper.

3.4 Underlying technology

3.4.1 Kinetic Monte Carlo simulations of void lattice formation during irradiation

H.L. Heinisch (*Pacific Northwest National Laboratory, Richland, USA) and B.N. Singh*

Simulations of void lattice formation were performed using the Kinetic Monte Carlo (KMC) model, starting from a random array of small voids and introducing randomly positioned crowdion and vacancy clusters that interact with the voids. Periodic boundaries are imposed, and the mobile defects interact only with the voids.

Many initial scenarios for void lattice formation from a set of randomly distributed voids were explored before success – quantifiable void ordering – was achieved. An initial minimum density of small, randomly-positioned voids seems to be a prerequisite for forming a void lattice. Starting with a low density of random large voids will lead to a void lattice only if the voids can be efficiently moved into position by collisions or destroyed and regrown, which are highly unlikely processes in such a situation where the shadow effect of already aligned voids is weak. The most likely scenario starts with a high enough concentration of small voids that there is a small void very near every position a lattice void will occupy. Then, by the shadow effect, the crowdion clusters will select the lattice, destroying the voids not in lattice positions and allowing the others to grow.

In radiation experiments void lattices are observed to form in small local regions of ordering which grow in extent with increasing dose. This implies that initial ordering takes place locally, perhaps as a result of the shadow effect caused by one significantly larger void (or perhaps two or more large voids correlated along a close-packed direction) occurring as a result of statistical fluctuations. To test this, simulations were performed in a fcc cell with a cube edge of 120 atomic lattice parameters, starting with a 1000 small voids and a "seed" consisting of 14 much larger voids arranged in a fcc super-lattice. Simulations were also done with the same initial conditions but with a seed consisting of a single large void in the center of the cell, and also with no seed. After irradiating with 6×10^5 crowdion clusters with n_{dc} (the number of hops made between direction changes) = 2×10^4 hops and 5×10^5 vacancy clusters, very similar ordered lattices of voids were produced in all three cases, but with a void lattice parameter somewhat smaller than that of the 14 void seed. Figure 12 shows the initial configuration and the ordered configuration after irradiation in the simulation with no seed. In the cells with seeds, the irradiation caused the seed voids to dissolve or move to fit the smaller void lattice parameter, and they became indistinguishable from the other lattice voids.

By simulating the formation of void lattices in idealized KMC models, we have attempted to determine the microstructure conditions and cluster kinetics under which void lattices can form and to relate this information to experimental measurements of the spacing of void lattices and the void size. In this way, void lattice experiments may provide a direct link, through the KMC modeling, for investigating characteri-stics of the primary defect production.

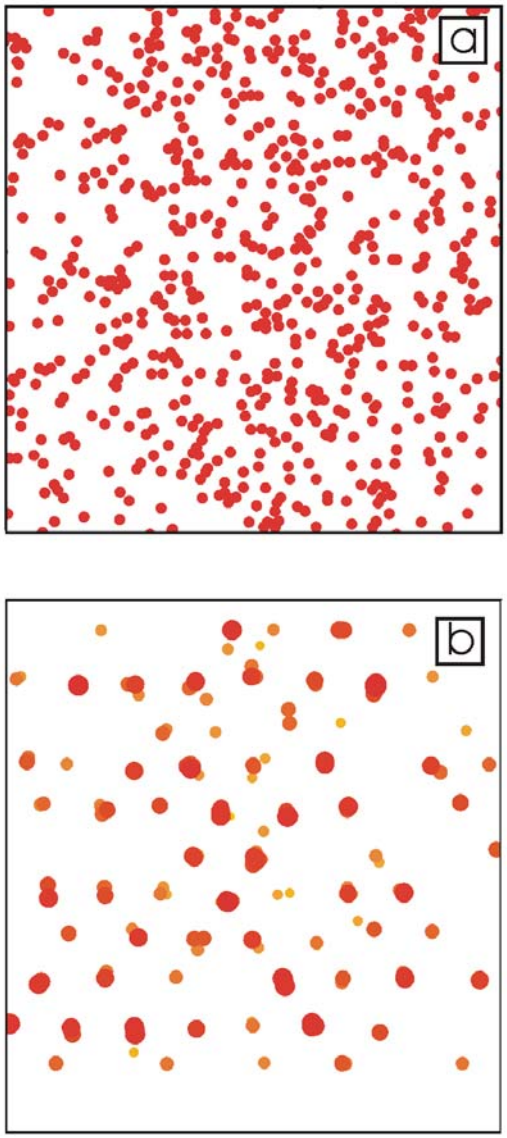

Figure 12. Results of KMC simulation of void lattice formation during irradiation: (a) initially, small voids are randomly placed within a cubic volume, (b) after irradiation by 1-D migrating interstitial clusters and 3-D migrating vacancies void lattice is formed.

3.4.2 Plastic flow localization in neutron-irradited copper and CuCrZr alloy

B.N. Singh, D.J. Edwards[*] ([*]Pacific Northwest National Laboratory, Richland, USA) and P. Toft

The phenomenon of plastic flow localization has frequently been observed in neutron-irradiated metals and alloys for almost 40 years. The localized deformation occurs in narrow channels (50 – 300 nm) by the glide of dislocations along a limited slip system, effectively annihilating the defect clusters produced during irradiation and producing soft "cleared" channels while the surrounding matrix is virtually undeformed. So far, very little is known about the mechanisms involved in the channel initiation and propagation during post-irradiation deformation. On the other hand, the localization of the plastic flow in these channels may be responsible for causing the yield drop and plastic instability in the neutron-irradiated materials. This is a matter of serious concern from the point of view of performance and lifetime of materials used in the structural components in fission or fusion reactors. The present work was initiated to address this problem by carrying out some specific experiments to determine (a) the sites at which these channels are initiated and (b) the frequency of these channel formation on the applied strain during a tensile test carried out at a constant strain rate.

Tensile specimens of OFHC-copper and CuCrZr alloys were irradiated with fission neutrons at 373K to a displacement dose level of ~0.3 dpa and tensile tested at the irradiation temperature. A second set of OFHC-copper tensile specimens were irradiated at 323K to a dose level of 0.3 dpa. These specimens were used for "interrupted" tensile tests at 295K. In this series of tests, an individual specimen was loaded in tension to a certain pre-determined stress/strain level and then unloaded for microstructural investigations. Four such "interrupted" tests were performed on five different irradiated specimens by unloading the specimens at (a) a stress level prior to the upper yield stress, and at plastic strain levels of (b) ~1%, (c) ~5% and (d) ~11%. The corresponding stress-strain curves are shown in Fig 13. The fifth specimen was loaded until the specimen fractured into two pieces. The specimen fractured at a strain level of ~20%.

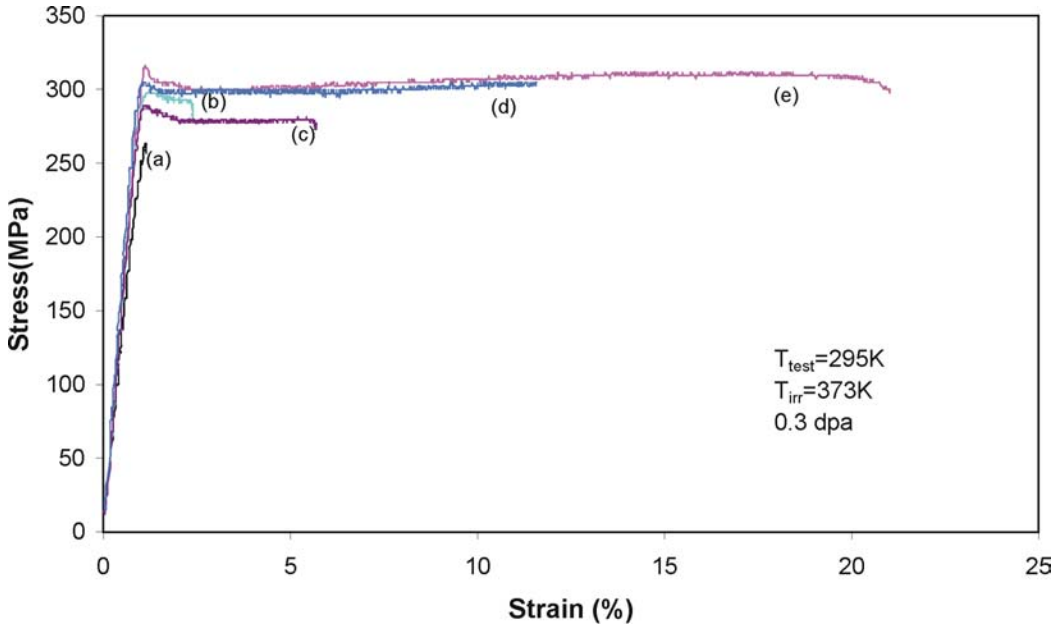

Figure 13. Stress-strain curves for the interrupted tensile tests on copper specimens irradiated at 323K to 0.3 dpa and tested at room temperature.

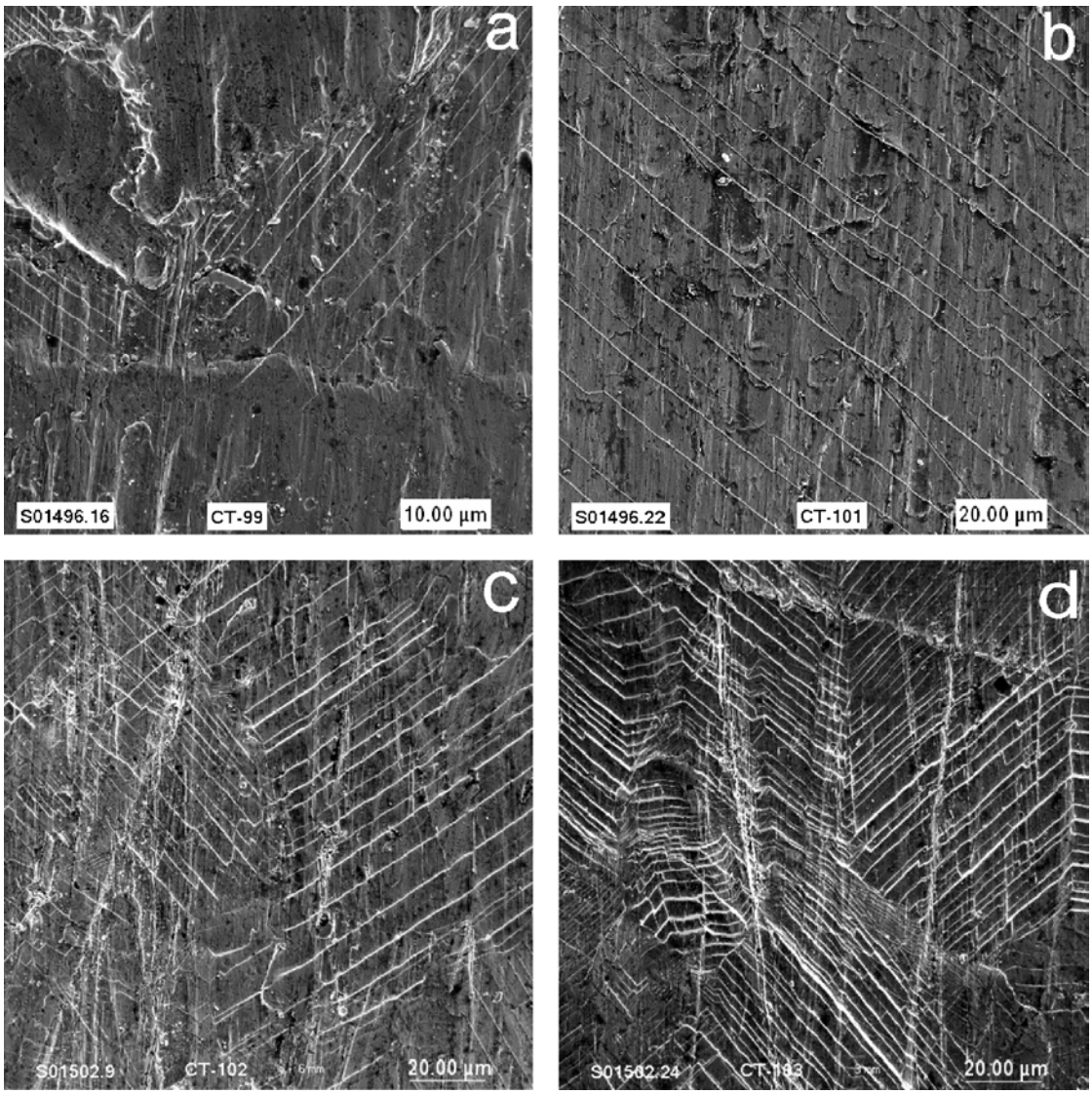

Figure 14. Scanning electron micrographs showing the presence of deformation bands on the surface of irradiated (0.3 dpa, 323K) copper specimens deformed to different strain levels: (a) in the elastic regime, (b) ~1%, (c) 5%, and (d) ~11%. Note that the number of deformation bands formed increases with increasing strain level.

In order to determine the evolution of deformation induced microstructure, all five specimens were investigated using transmission and scanning electron microscopes. Figure 14 shows the results of the scanning electron microscopy on the surface of specimens loaded to different strain levels. The white lines on these micrographs represent deformation bands (i.e. cleared channels) formed during the tensile loading. It is interesting to note that the irradiated specimens begin to show the formation of deformation band (a clear indication of flow localization) already in the elastic regime (i.e. before the initiation of plastic deformation). Furthermore, the number of such deformation bands formed during straining increases with increasing strain (stress) level. The important implication of these observations is that the plastic deformation continues to occur in a localized fashion throughout the whole deformation regime until the specimen fractures. This behaviour is confirmed by the transmission electron microscopy results. The transmission electron microscopy results show further that while the deformation continues in a localized fashion, there is no indication of homogeneous deformation between these deformation bands (Fig. 15). In other words, the

localized mode of deformation dominates the plastic behaviour of copper irradiated at low temperatures. Microscopy results clearly suggest that the clear channels are invariably initiated at grain boundaries, twin boundaries, interfaces and even clear channels themselves.

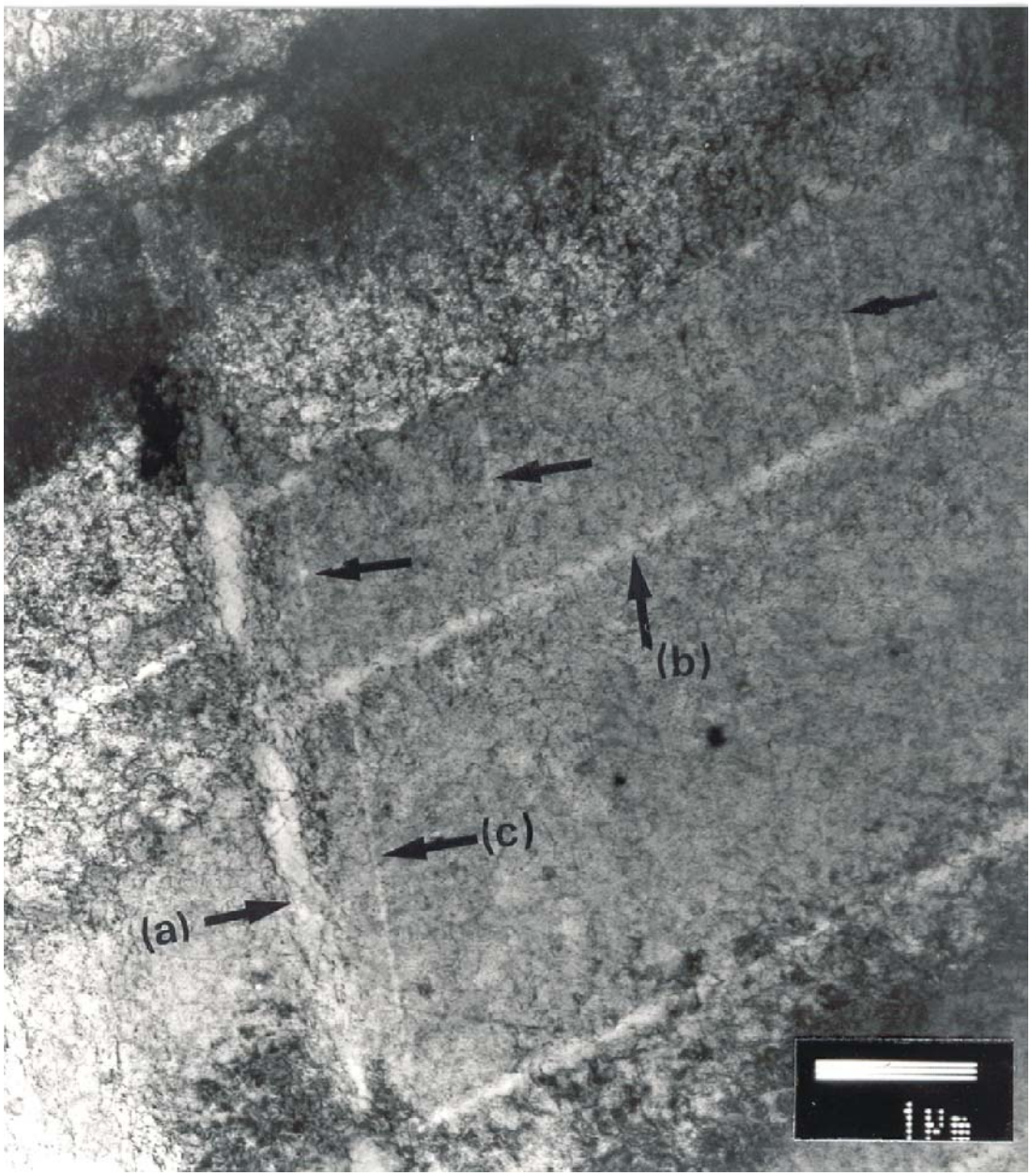

Figure 15. Transmission electron micrographs showing the formation of cleared channels in an irradiated (373K, 0.3 dpa) and deformed (at 22°C) copper specimen. Channels are formed at different stages during deformation (see differences in channel width).

3.4.3 Post-irradiation annealing of neutron irradiated OFHC-copper

B.N. Singh, D.J. Edwards[*] ([*]Pacific Northwest National Laboratory, Richland, USA) and M. Eldrup

Over the years, experimental observations have established that the primary damage production in copper during neutron irradiation is dominated by the collapse of vacancies in the centre of neutron-induced cascades in the form of a cluster of vacancies known as stacking fault tetrahedron (SFT). These SFTs arre very stable both configurationally and thermally. As a result, their density increases very rapidly with irradiation dose and reached a very high value at temperatures below the recovery stage V (i.e. 0.4 T_m, where T_m is the melting temperature). This means that kinetics of the damage accumulation in this temperature range is totally dominated by the high density of these SFTs. Since practically nothing is known about the thermal stability of SFTs, one always has to make some arbitrary and ad hoc assumptions about the thermal stability while calculating the temperature dependence of microstructural evolution. This is not a very satisfactory situation and to overcome this problem (at least in part) we have initiated experimental investigations to determine the annealing kinetics of SFTs.

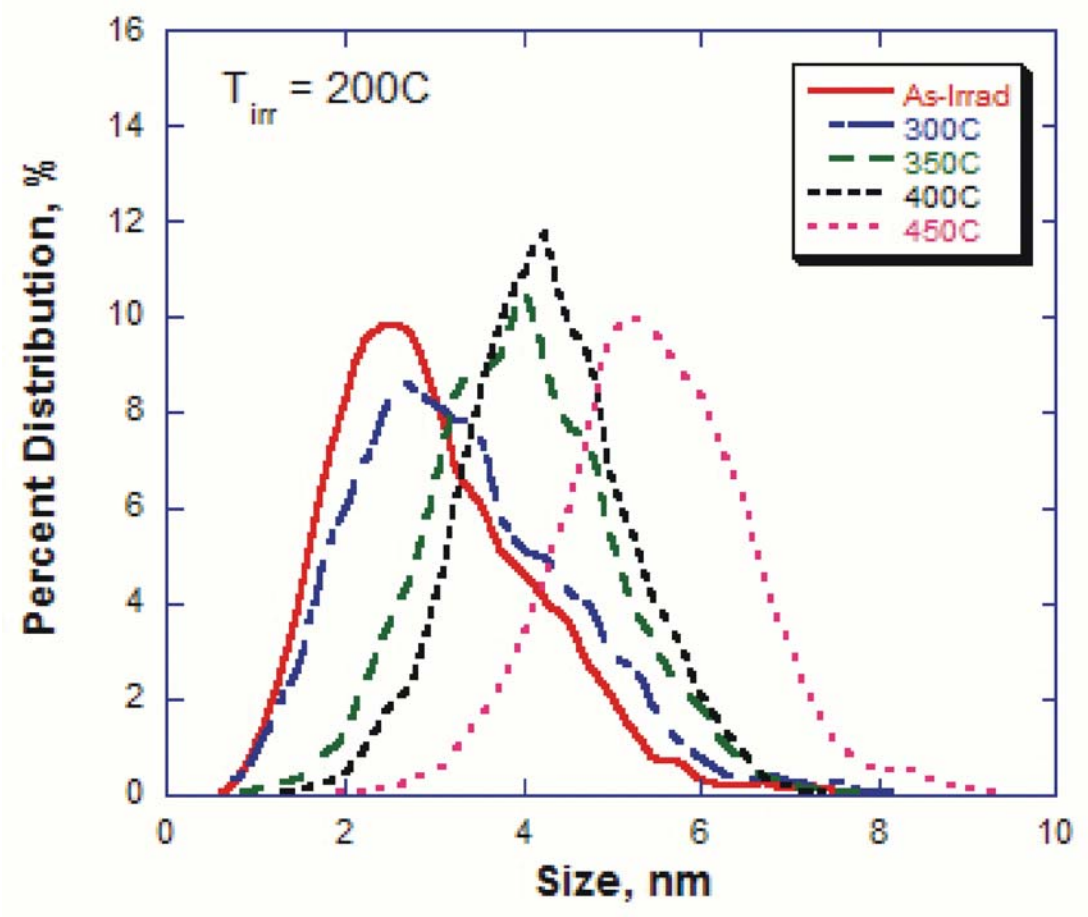

Figure 16. Size distributions of stacking fault tetrahedral (SFTs) in copper irradiated at 200°C to 0.3 dpa and annealed at different temperatures for 2 hours.

A number of tensile specimens annealed at 550°C for 2 hours were irradiated in the DR-3 reactor at Risø at 200°C to a dose level of ~0.3 dpa. For the present investigations, the irradiated specimens were annealed in vacuum at 300, 350, 400 and 450°C for 2 hours. Thin foils were prepared from the as-irradiated as well as from the post-irradiation annealed specimens and were examined in the JEOL 200FX transmission electron microscope at Risø.

Figure 16 shows the size distributions of SFTs determined from the TEM micrographs taken for the as-irradiated and post-irradiation annealed specimens. The mean size and average density of SFTs are quoted in Table 1. As it can be seen from Fig. 16, the annealing kinetics of the SFTs is enhanced by increasing the annealing temperature. The results quoted in Table 1 show that the major effect of annealing is on SFT density. The annealing at 450°C for 2 hours reduces, for instance, the SFT density be a factor of about 18 with a less than a factor of two increase in the mean SFT size. These results clearly demonstrate that with increasing annealing temperature, the net loss of vacancies from the SFTs increases. These results will be analysed in detail to determine the mechanism controlling the annealing kinetics of SFTs.

Table 1. Size and density of stacking fault tetrahedra in OFHC-copper in the as-irradiated (at 200°C to 0.3 dpa) and post-irradition annealed conditions. Post-irradition annealing was carried out for 2 hours at 300, 350, 400 and 450°C.

Annealing Condition	**Mean Size (nm)**	**Average Density ($10^{23}/m^{-3}$)**
As-irradiated	3.10	3.00
300°C/2 h (annealed)	3.43	2.05
350°C/2 h "	4.12	0.68
400°C/2 h "	4.39	1.03
450°C/2 h "	5.61	0.17

3.5 Publications and conference contributions

3.5.1 International publications

Edwards, D.J.; Singh, B.N.; Xu, Q.; Toft, P., Post-irradiation annealing of neutron irradiated CuCrZr. J. Nucl. Mater. (2002) v. 307-311**,** Pt. 1 p. 439-443

Eldrup, M.; Singh, B.N.; Zinkle, S.J.; Byun, T.S.; Farrell, K., Dose dependence of defect accumulation in neutron irradiated copper and iron. *J. Nucl. Mater.* (2002) v. 307-311, Pt. 2 p. 912-917

Ghoniem, N.M.; Tong, S.H.; Huang, J.; Singh, B.N.; Wen, M., Mechanisms of dislocation-defect interactions in irradiated metals investigated by computer simulations. J. Nucl. Mater. (2002) v. 307-311, Pt. 2 p. 843-851

Heinisch, H.L.; Singh, B.N., The effects of one-dimensional migration of self-interstitial clusters on the formation of void lattices. J. Nucl. Mater. (2002) p. 307-311, Pt. 2 p. 876-880

Kalinin, G.M.; Fabritziev, S.A.; Singh, B.N.; Tähtinen, S.; Zinkle, S.J., Specification of properties and design allowables for copper alloys used in HHF components of ITER. J. Nucl. Mater. (2002) v. 307-311**,** Pt. 1 p. 668-672

Osetsky, Y.N.; Bacon, D.J.; Singh, B.N., Statistical analysis of cluster production efficiency in MD simulations of cascades in copper. J. Nucl. Mater. (2002) v. 307-311, Pt. 2 p. 866-870

Osetsky, Y.N.; Bacon, D.J., Singh, B.N.; Wirth, B., Atomistic study of the generation, interaction, accumulation and annihilation of cascade-induced defect clusters. J. Nucl. Mater. (2002) v. 307-311, Pt. 2 p. 852-861

Schiøtz, J.; Leffers, T.; Singh, B.N., Modeling of dislocation generation and interaction during high-speed deformation of metals. Radiat. Eff. Defects Solids (2002) v. 157 p. 193-200

Singh, B.N.; Eldrup, M.; Zinkle, S.J.; Golubov, S.I., On grain-size-dependent void swelling in pure copper irradiated with fission neutrons. Phil. Mag. A (2002) v. 82 p. 1137-1158

Singh, B.N.; Ghoniem, N.M.; Trinkaus, H., Experiment-based modelling of hardening and localized plasticity in metals irradiated under cascade damage conditions. J. Nucl. Mater. (2002) v. 307-311, Pt. 1, p. 159-170

Trinkaus, H.; Singh, B.N., Modeling of void nucleation under cascade damage conditions. J. Nucl. Mater. (2002) v. 307-311, Pt. 2, p. 900-906

Trinkaus, H.; Heinisch, H.L.; Barashev, A.V.; Golubov, S.I.; Singh, B.N., 1D to 3D diffusion-reaction kinetics of defects in crystals. *Phys. Rev. B* (2002) v. 66, p. 060105.1-060105.4

Tähtinen, S.; Moilanen, P.; Singh, B.N.; Edwards, D.J., Tensile and fracture toughness properties of unirradiated and neutron irradiated titanium alloys. J. Nucl. Mater. (2002) v. 307-311, Pt. 1 p. 416-420

Tähtinen, S.; Laukkanen, A.; Singh, B.N.; Toft, P., Properties of copper–stainless steel HIP joints before and after neutron irradiation. J. Nucl. Mater. (2002) v. 307-311, Pt. 2, p. 1547-1553

Zinkle, S.J.; Hashimoto, N.; Hoelzer, D.T.; Qualls, A.L.; Muroga, T.; Singh, B.N., Effect of periodic temperature variations on the microstructure of neutron-irradiated metals. J. Nucl. Mater. (2002) v. 307-311, Pt. 1, p. 192-196

3.5.2 Danish reports

Bindslev, H.; Singh, B.N (eds.), Association Euratom - Risø National Laboratory annual progress report 2001. Risø-R-1345(EN) (2002) 49 p. **Foreign books and reports**

Edwards, D.J.; Singh, B.N., Overaging og Outokumpu CuCrZr at 600 deg. C. In: Fusion materials. Semiannual progress report for the period ending December 31, 2001. DOE/ER-0313/31 (2001) p. 118-122

Edwards, D.J.; Singh, B.N.; Toft, P., True stress-strain behavior of as-irradiated and post-irradiation annealed pore copper. In: Fusion materials. Semiannual progress report for the period ending June 30, 2001. DOE/ER-0313/30 (2001) p. 99-108

Kleykamp H., Linke J., Lucas G.E. and Singh B.N. (Editors), Proceedings of the Tenth International Conference on Fusion Reactor Materials (ICFRM-10), *J. Nucl. Mater.* (2002) v. 307-311**,** pp 1790.

3.5.4 Unpublished conference contributions and lectures

Eldrup, M.; Singh, B.N., Accumulation of point defects and their complexes in irradiated materials - studied by the use of positron annihilation spectroscopy. 2. IEA fusion materials agreement workshop on modeling and experimental validation, Les Diablerets (CH), 30 Sep - 4 Oct 2002. Unpublished. Abstract available

Golubov, S.I.; Singh, B.N.; Trinkaus, H., Treatment of microstructural evolution under cascade damage conditions within the framework of production bias model: Status and perspectives. 2. IEA fusion materials agreement workshop on modeling and experimental validation, Les Diablerets (CH), 30 Sep - 4 Oct 2002. Unpublished. Abstract available

Heinisch, H.L.; Singh, B.N., Kinetic Monte Carlo simulations for the study of defect diffusion and microstructure evolution in irradiated materials. 1. International conference on multiscale materials modelling, London (GB), 17-20 Jun 2002. Unpublished. Abstract available

Singh, B.N., Plastic flow localization in neutron irradiated metals and alloys. Workshop on damage production and accumulation under cascade damage conditions, Liverpool (GB), 14-16 Jun 2002. Unpublished. Abstract available

Singh, B.N., Radiation hardening in copper alloys containing different types of precipitates. Workshop on damage production and accumulation under cascade damage conditions, Liverpool (GB), 14-16 Jun 2002. Unpublished. Abstract available

Singh, B.N., Defect accumulation and its impacts on properties of BCC crystals under cascade damage conditions. IEA workshop on ferritic martensitic steels, Garching (DE), 14 Nov 2002. Unpublished. Abstract available

Singh, B.N., Materials response to mono- and multi-atomic displacements. Meeting at Department of Mechanical and Aerospace Engineering, University of California, Los Angeles, CA (US), 24 Apr 2002. Unpublished. Abstract available

Singh, B.N., Modelling of materials response to irradiation induced defects and impurities. Meeting on modelling and experimental validation activities in the fusion materials long term programme, Villigen (CH), 26-27 Feb 2002. Unpublished. Abstract available

Singh, B.N., Effect of neutron irradiation on physical and mechanical properties of Fe and F82H steel. Monitoring meeting, EFDA, Garching (DE), 19-21 Feb 2002. Unpublished. Abstract available

Singh, B.N.; Ghoniem, N.M., Aspects of plastic flow localization: Experiments, theory and modelling. 9. International symposium on plasticity and its current applications (Plasticity '02), Aruba (AW), 3-8 Jan 2002. Unpublished. Abstract available

Trinkaus, H.; Singh, B.N., Helium accumulation in irradiated metals, where do we stand?. 2. IEA fusion materials agreement workshop on modeling and experimental validation, Les Diablerets (CH), 30 Sep - 4 Oct 2002. Unpublished. Abstract available

Zinkle, S.J.; Singh, B.N.; Edwards, D.J., Origin and evolution of flow localization in metals: Assessment of experimental observations. 1. International conference on multiscale materials modelling, London (GB), 17-20 Jun 2002. Unpublished. Abstract available.

Title and authors

Association Euratom – Risø National Laboratory
Annual Progress Report 2002

Edited by H. Bindslev and B.N. Singh

ISBN	ISSN
87-550-3225-7 87-550-3226-5 (Internet)	0106-2840; 1396-3449

Department or group	Date
Optics and Fluid Dynamics Department	May 2003

Pages	Tables	Illustrations	References
53	1	28	15

Abstract (max. 2000 characters)

The programme of the Research Unit of the Fusion Association Euratom - Risø National Laboratory covers work in fusion plasma physics and in fusion technology. The fusion plasma physics research focuses on turbulence and transport, and its interaction with the plasma equilibrium and particles. The effort includes both first principles based modelling, and experimental observations of turbulence and of fast ion dynamics by collective Thomson scattering. The activities in technology cover investigations of radiation damage of fusion reactor materials. These activities contribute to the Next Step, the Long-term and the Underlying Fusion Technology programme. A summary is presented of the results obtained in the Research Unit during 2002.

Descriptors INIS/EDB

LASER DOPPLER ANEMOMETERS; MAGNETIC CONFINEMENT; NONLINEAR PROBLEMS; NUMERICAL SOLUTION; PELLET INJECTION; PHYSICAL RADIATION EFFECTS; PLASMA DIAGNOSTICS; PLASMA SCRAPE-OFF LAYER; PLASMA SIMULATION; PROGRESS REPORT; RISOE NATIONAL LABORATORY; THERMONUCLEAR REACTOR MATERIALS; TOKAMAK DEVICES; TURBULENCE; VORTICES